For Reference

NOT TO BE TAKEN FROM THIS ROOM

For Reference

NOT TO BE TAKEN FROM THIS ROOM

Ex LIBRIS
UNIVERSITATIS
ALBERTAENSIS

UNIVERSITY OF ALBERTA
QUAECUMQUE VERA

University of Alberta
Printing Department

Digitized by the Internet Archive
in 2018 with funding from
University of Alberta Libraries

https://archive.org/details/multicomponentin00coli

Thesis
1964
#19

THE UNIVERSITY OF ALBERTA

MULTI-COMPONENT INHIBITORS IN THE ACID CORROSION OF STEEL

A Thesis

Submitted to the Faculty of Graduate Studies

In Partial Fulfilment of the Requirements

for the Degree of Master of Science

DEPARTMENT OF MINING AND METALLURGY

by

COLIN DUNCAN

EDMONTON, ALBERTA

APRIL, 1964

ABSTRACT

The corrosion of low carbon steel coupon specimens has been studied at temperatures ranging from 60°C to 95°C both in the annealed and as- received condition. The corroding medium was aqueous hydrochloric acid, pH_1.

A re-evaluation of the inhibition offered by aliphatic amine, alcohol, carboxylic acid, sulfate and phosphate inhibitor molecules has been reported and the properties of combinations of these inhibitors studied.

These experimental results have been integrated with other findings from the general field of surface chemistry to verify a new approach, explaining the synergistic effect of multiple inhibitor systems, the Barrier Film Theory. The results reaffirm earlier observations of the beneficial effects of increased molecular weight on inhibition which are explained in terms of the new theory.

ACKNOWLEDGEMENTS

The author wishes to express his gratitude to Dr. J. Leja for his guidance and helpful criticism and to Dr. W.V. Youdelis for his assistance in interpreting the reaction rate data. The assistance of Mr. J. Wojno and Mr. R.M. Scott is also gratefully acknowledged.

The study has been made possible through the National Research Council grant A-699 and assistance received from the University of Alberta.

TABLE OF CONTENTS

	Page
INTRODUCTION	
General Remarks	1
Organic Inhibitors	2
Theory of Cathodic Inhibition	4
Barrier Film Theory of Inhibition	9
EXPERIMENTAL PROCEDURES	
Materials	18
Apparatus	20
Sampling	20
Pickling and Coupon Preparation	21
Acid Cleaning Glassware	23
Solution Preparation	23
Metallurgical Examination	26
Surface Tension Measurements	26
Weight-Loss Corrosion Tests	28
EXPERIMENTAL RESULTS	
Uninhibited Reaction Tests	32
General	32
Coupon Size	32
Temperature	32
Aging Time	34
Mixer Speed	34
Grain Structure	34
Time-Temperature Studies	36

Page

Inhibited Reaction Tests 42

General 42

Amine Evaluation 43

Critical Concentration for Inhibition 45

Evaluation of Surfactant Combinations 46

Time and Temperature Effects on Inhibited Corrosion 49

Miscellaneous Studies

Experimental Activation Energy - Uninhibited Reaction 55

Monomolecular Films 56

Static Water Drop Indicator Tests 58

Surface Tension Determinations 59

DISCUSSION

General 62

The Uninhibited Reaction 62

The Uninhibited Reaction Rates 63

The Inhibited Reaction 70

Amine Inhibitors 70

Multicomponent Inhibitors 72

CONCLUSIONS 75

REFERENCES 78

APPENDICES 81

LIST OF ILLUSTRATIONS

		Page
Fig. 1	Partial Adlineation of C_{14} Metal-Soap Film	I0
Fig. 2	Steric Hindrance in a Metal-Soap Film	I2
Fig. 3	Fully Adlineated, Compact, C_{14} Metal-Soap Film	I2
Fig. 4	Bonding Forces in a Multiple Inhibitor Film	I5
Fig. 5	Corrosion Test Apparatus	I9
Fig. 6	Drop Volume Surface Tension Apparatus and Thermostatic Bath	I9
Fig. 7	Oscilloscope Trace of Coupon Heating Time	3I
Fig. 8	Iron Oxide Film Growth	33
Fig. 9	Coupon Specimen	33
Fig. 10	Edge View of As-Received Lot No. 1 Coupon	35
Fig. 11	Edge View of Lot No. 1 Coupon Annealed in Argon 1.3 Hours at 820°C	35
Fig. 12	Uninhibited Weight-Loss Data - Pickled Specimens	37
Fig. 13	Uninhibited Weight-Loss Data - Pickled Specimens	38
Fig. 14	Uninhibited Weight-Loss Data - Specimens not Pickled	40
Fig. 15	Effect of Non-Polar Chain Length on Inhibition	44
Fig. 16	Critical Inhibitor Concentration	44
Fig. 17	Multicomponent Inhibition	47
Fig. 18	Inhibitor Film Life - Time and Temperature Effects	5I
Fig. 19	Inhibitor Film Life - Time, Temperature and Composition Effects	54
Fig. 20	Surface Tension of Homologous Carboxylic Acid Series	60

LIST OF ILLUSTRATIONS

		Page
Fig. 21	Critical Micelle Concentrations, 60°C, Amine and Multicomponent Inhibitors	60
Fig. 22	Edge view of As-Received Lot No. 2 Coupon Showing Shear Deformation, Oxide Film and Sulfide Inclusions	68
Fig. 23	Edge view of Lot No. 2 As-Received Coupon	69
Fig. 24	Edge view of Lot No. 2 coupon after 6 Hours Immersion at 80°C, Uninhibited	69
Fig. 25	Edge view of Lot No. 2 coupon after 6 Hours Immersion at 60°C, Inhibited C_{16} Amine	71
Fig. 26	Edge view of Lot No. 2 coupon, Annealed 1.3 Hours in Argon at 820°C, after 6 Hours Immersion at 60°C, Inhibited C_{16} Amine	71
Fig. 27	Frequency Distribution, Uninhibited Corrosion, Lot No. 2 Specimens, after 6 Hours Immersion at 60°C	88
Fig. 28	Arrhenius Plot of Experimental Corrosion Rate Data	111

LIST OF APPENDICES

		Page
APPENDIX A		
Table A-1	Typical Analysis of Coupon Specimens	81
APPENDIX B	STUDY OF THE VARIABLES AFFECTING THE UNINHIBITED CORROSION RATE	
Table B-1	Preliminary Evaluation - Lot No. 1 Specimens	82
Table B-2	Effect of Mixer Speed Students' t Test of Mixer Speed Data	83
Table B-3	Uninhibited Corrosion - Lot No. 2 Specimens	86
Table B-4	Frequency Analysis of Uninhibited Corrosion Rate - Lot No. 2 Specimens	87
APPENDIX C	EVALUATION OF THE EFFECT OF TEMPERATURE ON THE UNINHIBITED CORROSION RATE	
Table C-1	Uninhibited Corrosion Rate 60°C	89
Table C-2	Uninhibited Corrosion Rate 80°C	90
Table C-3	Uninhibited Corrosion Rate 90°C	91
Table C-4	Uninhibited Corrosion Rate 95°C	92
APPENDIX D	CORROSION OF UNPICKLED SPECIMENS	
Table D-1	Uninhibited Corrosion Rate 90°C	93
APPENDIX E	MISCELLANEOUS ESTIMATES	
E-1	Estimation of Shear Deformed Metal	94
E-2	Estimation of Oxide Mill Scale	95
E-3	Standard Chemical Potentials	96
E-4	Mill Scale Dissolution	97

LIST OF APPENDICES

		Page
APPENDIX F	STUDY OF THE EFFECTS OF TIME, TEMPERATURE AND INHIBITOR CONCENTRATION ON INHIBITED CORROSION RATES	
Table F-1	Comparison Between Mono and Di-Alkyl Amines and the Effect of Chain Length	100
Table F-2	Critical Inhibitor Concentration	101
Table F-3	Combined Amine and Carboxylic Acid Inhibition	102
Table F-4	Combined Amine, Carboxylic Acid and Alcohol Inhibition	103
Table F-5	Combined Amine, Acid, Alcohol and Sulfate Inhibition	104
Table F-6	Combined Amine, Sulfate and Amine, Phosphate Inhibition	105
Table F-7	Effect of Immersion Time and Temperature on Multicomponent Inhibition	106
Table F-8	Effect of Immersion Time, Temperature and Concentration on Multicomponent Inhibition	108
APPENDIX G	EXPERIMENTAL ACTIVATION ENERGY FOR UNINHIBITED CORROSION	110
APPENDIX H	SURFACE TENSION STUDIES	
Table H-1	Melting Point Determinations	113
Table H-2	Calibration of Drop Volume Surface Tension Apparatus	114
Table H-3	Determination of C.M.C. - C_{16} Amine Inhibitor	116
Table H-4	Determination of C.M.C. - Multicomponent Inhibitor	117

INTRODUCTION

GENERAL REMARKS

Corrosion is a phenomenon common to all metallic substances and involves a spontaneous conversion of elemental metal to a chemical compound which is more stable under the environmental conditions. Corrosive attack varies greatly from metal to metal, is dependent both on the environment and the reaction product, and is determined both by the free energy changes and the kinetics of the reactions involved in the given system.

Corrosion can be a desirable process, as in the case of the formation of protective aluminum and chromium oxides, or the destruction of sacrificial anodes used in the protection of sub-surface structures. As a rule, however, corrosion is an undesirable cause of rising industrial costs. In order to combat corrosion, a whole field of scientific activity is required to study the phenomena.

The available corrosion controls are limited to one or a combination of three approaches:

1. Removal of corrosive constituents from the environment, thereby creating an inert system,
2. Use of special alloys, properly selected and pretreated, to limit constituent corrosion-accelerators prevailing in the solid state or to provide protective (reaction product) films,
3. Creation of an inactive barrier, isolating the metal from its environment.

The present study is concerned with the barrier approach to corrosion mitigation. More specifically, it deals with the effectivness of a barrier

film of organic surfactant forming on a steel specimen through the mechanism of adsorption from aqueous acid solution. Experimental data are discussed together with the observations of several other investigators and a theory is proposed to explain the improved corrosion inhibition where multi-component inhibitor systems are employed.

Contributions of information from researches in the field of flotation (molecular orientation, selectivity and reagent combinations), hetrogeneous catalysis (catalytic poisoning, coordination forces of adsorption) and surface chemistry in general (micelle formation, wetting, liquid-air and liquid-solid interface studies) have found useful application in the understanding of the possible mechanisms of inhibition.

ORGANIC INHIBITORS

Understanding of the mechanism of corrosion mitigation through the application of organic inhibitors has progressed from the dark ages to a period of relative enlightenment in a brief span of some fifty years. It is, however, entirely possible that ancient man was aware of the beneficial properties of animal fats in preserving his favorite implements, but modern understanding was prompted through a desire to economically improve the acid pickling of steel.

The pickling process is required to remove, through acid dissolution, the unsightly mill-scale on hot rolled steel. The principal method involved dipping the scaled metal into a hot acid bath. The scale was ultimately removed by direct dissolution or was peeled from the host metal substrate during the acid attack. Unfortunately, in either of these mechanisms, as the clean metal surface became exposed to the acid, an appreciable quantity

of sound metal was also dissolved. This unwanted dissolution was uneconomical both from the standpoints of metal loss and extra acid consumption. There was, therefore, an economic impetus to reduce both the loss of sound metal and the consumption of extra acid, and also to limit the unhealthy acid spray which was driven into the working area surrounding the pickling baths.

Exotic preparations such as glue, sumac leaves and jelly [1] were found successful, and the earliest investigators unwittingly launched the inhibitor studies which continue to the present day.

According to the electrochemical theory of the corrosion mechanism, corrosion takes place wherever there is a potential difference and a closed-circuit path for the necessary transfer of charges across the metal-solution interface [2,50a]. The first explanations of the effect of inhibitors on the corrosion mechanism were unavoidably based on the precepts of electrochemical theory, viz.,

1. Increased resistance due to a non-conducting surface film interposed between electrode and electrolyte or
2. Interference with either anodic or cathodic electrode processes, i.e. polarization effects, such as:
   (i) increased hydrogen overvoltage
   (ii) concentration polarization at either electrode and
   (iii) activation polarization.

Study of inhibition has included inorganic, organic, oxidizing and polar-nonpolar compounds. The inhibitive mechanism of inhibitor species was considered to be strictly electrical, i.e. charged species were electrostatically attracted to charged surface sites, (e.g.: a piece of iron in an acid

environment will be negatively charged, due to accumulated electrons provided by dissolution of iron in attaining equilibrium, and will then attract positively charged colloids or ions in solution). However, another view has accepted the overall adsorption of inhibitors to be a result of weak physical forces only[3a,4,5]; this theory is herein modified to include stronger chemical forces (covalent bonds) between inhibitor and specific surface points as well as lateral bonding between the inhibitor molecules themselves.

Organic inhibitors are almost unlimited in number and variety; initially, only aliphatic and heterocyclic amines and carboxylic acids were known, but alkyl-phosphates, - sulfates, - sulphonates, thiols, mercaptans, and many others are now finding useful application.

THEORY OF CATHODIC INHIBITION

An early theory of inhibition was proposed by Chappel et al,[1] who studied cathodic and anodic polarization of iron in inhibited N sulfuric acid. They concluded that the inhibition was due to adsorption on cathodic metal sites. Other investigators agreed with this conclusion and Mann[6] proposed a comprehensive theory of inhibition. The principal features of this early theory[6,7,8,9] consisted of the postulate that the effective organic inhibitors formed positive ions or positively charged colloids and these cations were attracted electrostatically to the cathodic regions, discharged and adsorbed to form a neutralised blanket film. Their function, once adsorbed, was to interfer with hydrogen discharge by offering a diffusion barrier appearing as a resistance in series to the flow of electrons. The extent of adsorption, the size of the molecules (and therefore the surface area covered) and the closeness of packing, were recognized as factors effective in corrosion

mitigation. Molecules were believed to sweep around a fixed point on the surface to which they were attached by the functional group, e.g. the amine nitrogen atom.

Organic inhibitors were thus first considered to offer protection as a result of increased resistance to charge transfer across the interface. Experimental justification was found in anodic and cathodic polarization tests showing changes in inhibitive power as the concentration and molecular structures of the various inhibitors were changed. Measurements of film resistances were contradictory, but apart from this, the polarization studies showed that inhibition at the high current densities and large negative potentials employed, was truly cathodic in nature; anodic processes appeared to be unaffected. These conditions are undoubtedly not reproduced in the open circuit corrosion conditions and erroneous conclusions were, therefore, not unlikely to be drawn.

The essential point in the cathodic adsorption theory is the attraction of positively charged particles to the negatively charged sites. However, in following this argument, one might consider, as did Machu[4], the pickling reaction. The ferric oxide scale in contact with steel is cathodic to the bare metal[50b]. If, as was proposed, inhibition was purely cathodic in nature, why was there no accelerated metal loss in the inhibited pickling baths since the bare metal would be unprotected? Machu suggests an overall adsorption of inhibitor on both anodic and cathodic sites with weaker reversible adsorption on the oxide scale allowing acid penetration to those regions, while stronger adsorption on the metal allowed a barrier film to protect the sound metal surfaces.

Additional evidence is available to put the cathodic theory in poor

light. Observations have been made which demonstrate conclusively that there is a shift in potential (open circuit) in the cathodic direction upon the addition of inhibitors[10]. To account for this, anionic properties would have to be ascribed to the inhibitor so that it could affect the anodic reaction. Using the cathodic theory, this behavior would require the reduction of inhibitor molecules and the associated transfer of electrons from the surface, thereby decreasing the magnitude of the negative potential - in other words, depolarization of the cathode. This seems an unlikely explanation since inhibitors showing cathodic shift are not reducible under corrosive conditions.

At small current densities, polarization studies have, in fact, shown dual anodic and cathodic behavior of inhibitors as well as purely anodic or cathodic properties. Hackerman and associates[10,11] among others[3b,12,13,14,15,28] have demonstrated the dual nature of aliphatic amines and in some instances a largely anodic behavior has been indicated, clearly a departure from the cathodic theory.

Another observation which cannot be resolved by the cathodic theory involves the specific nature of the organic adsorption[16,17,18,19,39]. Since, according to the theory, adsorption is electrostatic in nature and therefore completely general, it provides no explanation for the better inhibition occuring with sulfur compounds as compared to amines, despite the fact that in acid solutions, amine inhibitors are completely ionized, while the dissociation of sulfur compounds is restricted. Nor can it explain the decidedly specific adsorption found by Hackerman and Cook[16,17] in comparing carboxylic acid, alcohol, ester and amine type inhibitors. The acids, alcohols and esters adsorbed irreversibly on the same sites while amines adsorbed on different surface sites. This adds weight to any proposal that surface forces other than

merely electrostatic ones are operative.

Similarly, the specific effects of organic inhibitors on different metal surfaces cannot be explained by purely electrostatic forces of adsorption. Thiourea protects aluminum but has no effect on zinc and accelerates cadmium corrosion[20]. Further, due to the electrostatic nature of adsorption, if the cathodic theory were correct, one would expect an increased temperature to be harmful to all inhibited systems. This is true in some cases and not in others[10,21,22].

Early investigators were not only relying on the electrostatic adsorption and increased hydrogen overvoltage to explain inhibition but also leaned heavily on surface coverage or projected molecular area to explain inhibition. Mann[6,7], recognizing increased inhibitive power as the molecular weight and the number of substituent methyl groups were increased, believed that the effectivness was influenced by the area of the molecule projected on the surface. Swearingen and Schram[23] and Hackerman et al[24,25] found, however, that a series of cyclic amines and imines having approximately equal cross sectional area exhibit very divergent inhibitive properties. This, then, provided added support to the belief that specific adsorption is an important aspect of inhibition. Steric effects have been well studied[26,27,28] and, for instance, the ortho substitution of a methyl group had been found to have beneficial effects on the inhibition offered by heterocyclic nitrogen compounds. More recently, Foster, Oakes and Kucera[29] carried out weight-loss tests on mild steel in solutions of hydrochloric acid inhibited by various substituted forms of propargyl alcohol

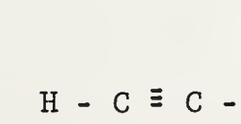

The triple bond was believed to be the effective portion of the molecule whose effectiveness could be modified through structural variations such as saturation of the triple bond; this was found to decrease the inhibitive value of the molecule. Substitution of the methine hydrogen by iodine, was also found to enhance the resulting inhibition. The conclusion was that the donor capacity of the triple bond was the key to the inhibitive properties.

The conclusion that might now be drawn, is that adsorption and the resultant inhibition are greatly affected by the molecular structure, not from the standpoint of surface area covered, but from considerations of the electron donor and acceptor properties of the molecules and their substituted forms.

The requirement of the cathodic theory of adsorption that inhibitors be positively charged is refuted by the excellence of o-tolylthiourea and sulfonated castor oil, neutral molecules in strongly acid solution but effective as inhibitors under these conditions[13].

Hackerman and Schmid [30] have shown the effectiveness of negatively charged inhibitors, while other papers[11,15,25,28] provide ample evidence of the anodic or both anodic and cathodic nature of other surfactants.

The difficulties encountered in the application of the cathodic theory are due to the rigid requirements of a positively charged colloid electrostatically adsorbed on a cathodic site. These difficulties can be obviated to a great extent by a more flexible approach to the possible adsorption mechanisms as derived from studies of surface chemistry.

THE BARRIER FILM THEORY OF INHIBITION

Polar organic molecules having electronegative (electron donor) elements such as sulfur, nitrogen, oxygen or unsaturated carbon bonds, have been found to adsorb strongly to metal substrates and to offer inhibition to corrosion. In heterogeneous catalysis, the adsorption of poisoning elements such as sulfur, takes place through the formation of coordination or donor linkage[31]. This bonding is made possible by the sharing of the unshielded electron pair of the donor sulfur, with the acceptor catalyst site. Supporting evidence was provided by the observed poisoning nature of carbon monoxide and cyanogen compounds. There is in this bonding, then, a logical parallel between the two phenomena - catalyst poisoning and inhibitor adsorption.

Formation of coordination bonding has been suggested by Hackerman[24,25] who found that by straining the normal nitrogen bonds in the imine molecule (on increasing the ring size), inhibition increased as a result of the increased exposure of the available, unshared, electron pair.

The formation of the coordination bonds leads to the suggestion, first made by Faraday[32], that semi or quasi compounds are formed on the surface between metal and chemisorbed molecules. This thought has also been expressed by others[28,33-36](some investigators suggesting the formation of a complex film and evidence of its existance has been shown[3d,37a]). These observations do not necessarily mean the absence of other forces (electrostatic or dipole-dipole) but merely show the possibility of stronger inhibitor-surface linkage.

There is little doubt that there are a variety of surface forces operating in adsorption, the nature of which depends on the surfactant, substrate and environmental condition. The metal surface itself is a mixture of active sites having a variety of intensities. The solid-state surface bonding in

Fig. I Partial Adlineation of C_{14} Metal-Soap Film

general is not completely satisfied since the requisite number of near neighbours are not provided. This leads to a modification of interatomic distances at the surface and an increased surface activity. The added features such as surface asperities, defects, grain-boundaries and impurities further create additional sites having varying degrees of activity. It is through adsorption that the unsatisfied bonds become partially satisfied, thereby reducing the excess energy available for reactions at points where adsorption has taken place.

Machu's[4] early proposal regarding orientation of inhibitor molecules and the later recognition of steric hindrance effects in adsorbed films, have received added support from studies of the solid-liquid and liquid-gas interfaces. Orientation of compact organic films has been found to be disrupted from the normal vertical arrangement by branching side chains as illustrated in Fig. 3 and film strengthening and solidification created through the use of long chain molecules have also been thoroughly studied[33,37b,38-43]. The supporting studies of the hydrophobic nature of adsorbed monolayer films, under varying conditions of pH, have shown that amine films are compact and strongly hydrophobic at low pH ranges due to the presence of strongly adsorbed and dissociated amine hydrochloride. The dissociated carboxylic acids form compact, hydrophobic films at a higher pH range[43]. Surfactants in combination have been found to associate in a regular fashion indicating a tendency to compound formation[33,37b,39], a proposal supported by the observation that liquid-expanded films of surfactants at the air-water interface exhibit solidification when a second reagent has been injected[37b]. All of these features indicate a bonding tendency between functional groups which could be utilized in strengthening an inhibitor film and add weight to recent observations of two component inhibitor adsorption and corrosion studies[16,27,28]. In these studies,

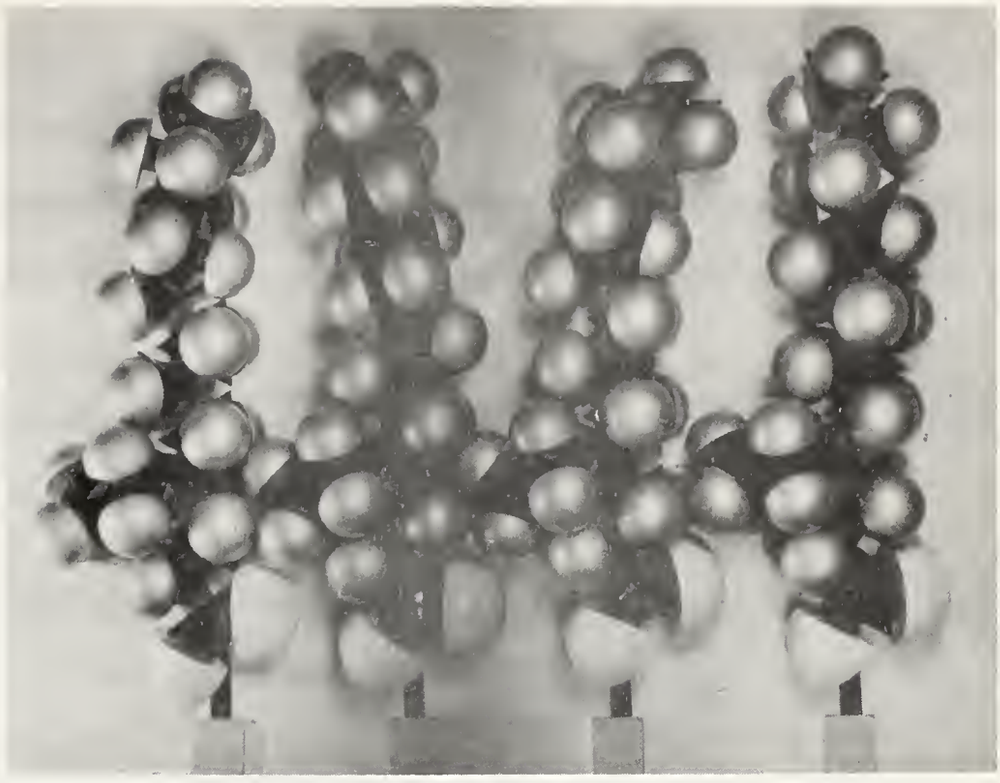

Fig. 2 Steric Hindrance in a Metal-Soap Film

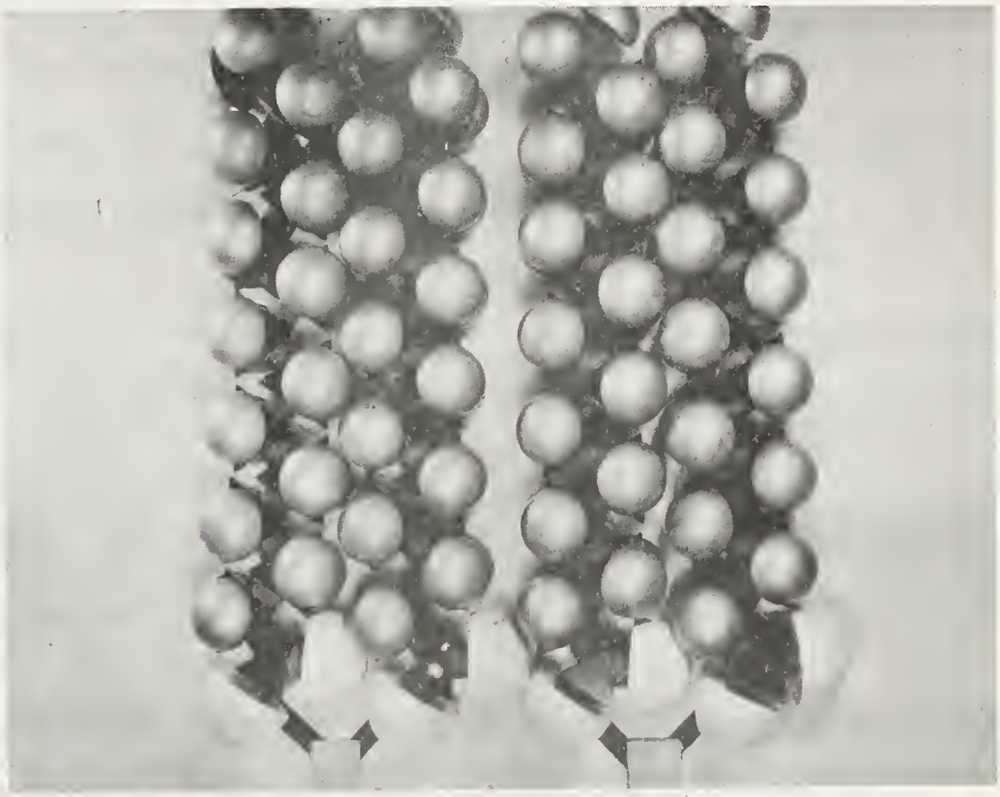

Fig. 3 Fully Adlineated, Compact, C_{14} Metal-Soap Film

the use of combined surfactants, each having a different polar group was found to decrease corrosion. Adsorption isotherms showed that the increased corrosion resistance was due to an increased irreversible adsorption creating a film covering a large surface area with a more rigid network of surface bonds.

The main features to be considered from these studies, which in turn form the basis of the Barrier Theory are these:

1. Organic molecules having electronegative functional groups are effective inhibitors and each is attracted to specific surface sites.
2. The hydrocarbon portion of such a molecule can be cyclic or aliphatic but a simple structure, preferably saturated, has been found to be most effective since the most compact film is then possible.
3. Mixed surfactants display film features such as attraction forces between functional groups which, if fully developed, could strengthen an inhibitor film.

The theory of the barrier film (Leja unpublished) thus proposes that a protective film can be created in situ at the metal/solution interface by a mixture of surfactant species capable of adsorption from the environment onto a metal surface. The film, in order to be protective, must display the following characteristics:

1. It must be firmly attached to withstand undermining forces such as exerted by flowing fluids and gas bubble impingement.
2. The film must be continuous in order to offer isolation to the metal from its environment. The film barrier must then prevent

diffusion of both metal ions and environmental species.

3. The film must be non-reactive with the environment or metal phase - in other words, it must not be a corrosion accelerator.
4. It must be capable of self-healing, a property made possible through the maintenance of an inhibitor reservoir in the corrosive environment.

These properties require that the inhibitor must consist of a polar group which is ionizable or possesses a dipole moment and a non-polar hydrocarbon chain. The use of a non-polar molecule would not in itself provide any degree of protection since highly polar H_2O, OH^- or Cl^- would be the preferred species adsorbing on any polar metal or reaction product on the surface. However, if a non-polar molecule is used in combination with surface active species, it could act as a solidifying agent for the adsorbed film, being held in place by the weak but multiple Van der Waals bonding forces between the hydrocarbon chains.

The bonding forces offered by three species of inhibitor are illustrated in Fig. 4. Three distinct bonding forces are apparent. The required firm attachment is provided by bonds I. They must be sufficiently strong at scattered sites to prevent undermining of the film.

Clear evidence of specific adsorption (chemisorption) of inhibitors at different sites has been reported, indicating the necessary film anchorage. The next step in the barrier film formation is the incorporation into the film of a number of other surfactants having differing functional groups. The result is a solidified complete monolayer coverage of inhibitor molecules strongly bonded to the surface.

I - forces between the polar functional group of the inhibitor and active metal surface sites.

II - interaction between the adjacent polar portions of the inhibitor molecules

and

III - the multiple Van der Waals forces existing between adlineated non-polar portions.

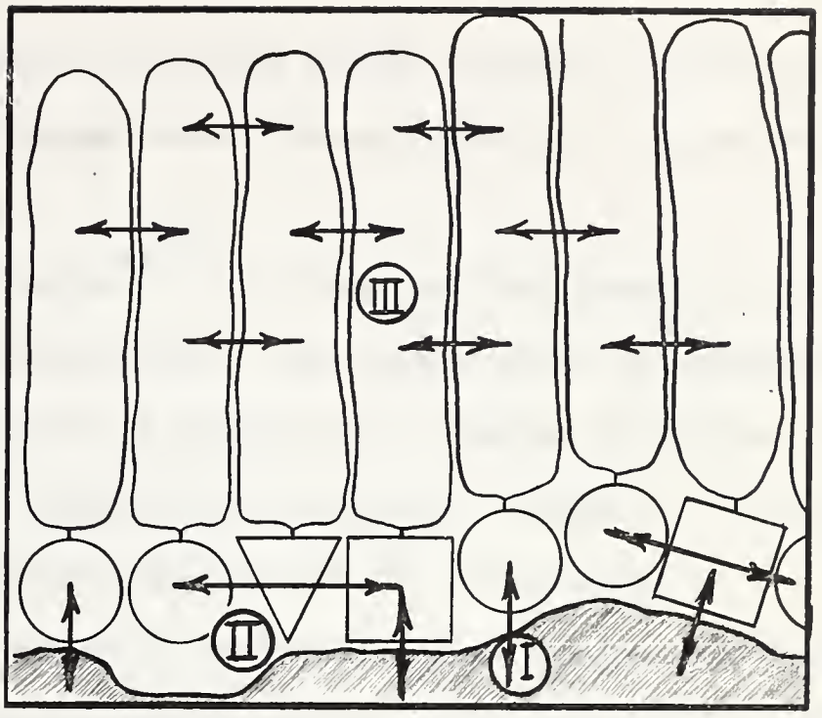

FIG. 4 BONDING FORCES IN A MULTIPLE INHIBITOR FILM

Recognition must be made, however, of the fact that effective inhibition will be affected by the solubility of the inhibitor - metal quasi-compound. The inhibitor bond must not be strong enough to dislodge the surface metal atom or atoms and hence, the criterion for point 3 in the list of desirable characteristics (Figs. 1,4).

The continuity and impenetrability of the film are provided by the multiple Van der Waals forces[43,39] III and assisted by forces II acting between functional polar groups.[33,37b,39,46] These forces will only come into play if sufficient film pressure is provided to cause adlineation of the non-polar chains. The forces will not be particularily strong unless the chains are of sufficient length to provide the multiple bonds. In this light then, the effects of steric hindrance become at once apparent, as illustrated in Fig. 3 . This approach explains the earliest observation that increased molecular weight increases the inhibition attained with many inhibitors. The

reason was that the resultant film was more tightly bonded, solidified and thereby created a much more impenetrable diffusion barrier. These bonds will satisfy requirement number 2.

Flotation[33] and lubrication[18,37c] studies have both brought out the synergistic action of mixed surfactants. Leja (unpublished) has suggested that an analogous behavior should be expected with combined inhibitors. In the light of these and other references to synergistic behavior, its application to the corrosion phenomena would undoubtedly be beneficial.

In summary then, the theory of the barrier film proposes that through the simultaneous use of properly selected surface active molecules possessing different polar groups, a greater number of active surface sites become host to inhibitor molecules. The film, strongly bonded to the surface, is further strengthened and densified by bonds between the functional groups and, in addition, by multiple Van der Waals bonds between the hydrocarbon portions of the inhibitor molecules. At a minimum concentration sufficient molecules are present to form a solidified adlineated film, strongly bonded to the surface and offering a rigid barrier which can bridge over microscopic surface depressions or areas on which no strong surface bond is developed (Figs. 1-4). The maintenance of a reservoir of surfactant in solution provides repair material in case the film becomes damaged in service.

The electrical effects of such a barrier film can be readily visualized. It would indeed affect both the anodic and cathodic regions of the metal surface, increasing the hydrogen overvoltage and creating both concentration and activation polarization effects. What might now become apparent is that the earlier descriptions of inhibition were being based on the effects rather than the cause of the inhibition mechanism.

The present study was undertaken to provide experimental evidence of the synergistic behavior of multicomponent inhibitors systems, as determined by weight loss tests. Of necessity, the study is limited to aliphatic molecules under a limited set of conditions of temperature and acidity.

EXPERIMENTAL PROCEDURES

MATERIALS

Coupons used in the weight-loss corrosion tests were all sheared from standard, rolled, 20 guage sheet metal stock, 36 inches by 96 inches. A typical analysis is shown in Table A-1. The coupons, as-received, carried unacceptable macroscopic surface blemished and thus an initial sorting was done in order to eliminate this as a source of future difficulties in reagent evaluation.

Water used in the preparation of reaction solutions was distilled once through a Barnstead all-tin still. The product normally ran from one to three ppm impurity expressed as sodium chloride according the the Industrial Instruments model Rd 3 conductivity meter.

Hydrochloric acid used in the reaction solutions and pickling bath was reagent grade as was the sulfuric acid used in the cleaning solutions.

All inhibitor reagents used were of 90 to 95% purity and were purchased from K and K Laboratories and Distillation Products Industries, a division of Eastman Kodak. No further purification procedures were carried out and thus their properties were not completely those of the pure compound. (See Table H-1 for melting point data.) A commercial orthophosphate was also evaluated but no purity data are available. The product was called mono-di tridecyl orthophosphate and was claimed to be an equi-molar mixture of the two phosphates.

Fig. 5 Corrosion Test Apparatus

Fig. 6 Drop Volume Surface Tension Apparatus and Thermostatic Bath

APPARATUS

As shown in Fig. 5 the reaction vessel, condenser, heating mantles and magnetic stirrer are all standard laboratory equipment. The balance used in these studies was a Mettler Micro-Gram-atic. The surface tension apparatus, (Fig. 6) built in the laboratory by Mr. J. Wojno, was operated in conjunction with a Colora, Ultra Thermostat type NB thermostatic bath.

Melting point determinations were carried out using a Leitz Wetzlar Microscope with heating stage adaptable to -20° to $+350^{\circ}$C.

Small five ml beakers supplied for the Beckman Zeromatic pH meter were used as weighing dishes for the surfactants.

Additional apparatus used was:

1. A General Radio type 631-BL Strobotac
2. A Mamco model 12500 heat gun
3. Glass Col heating mantles
4. Labline Magnestir No. 1250 magnetic mixers
5. Superior Electric type 116L Powerstats.

SAMPLING

As mentioned earlier, samples having surface blemishes (scratches, rust marks, etc.) were rejected. The remainder were measured by vernier caliper. Replicate measurements showed that specimen widths varied widely. The length dimension and thickness (original sheet guage) were consistent to $\pm$ 0.01 cm. The specimens were divided into the following three groups on the basis of the width dimension.

	THICKNESS	X	LENGTH	X	WIDTH
	(in centimeters)				
a.	0.153 ± 0.005		3.82 ± 0.010		1.28 - 1.31
b.	0.153 ± 0.005		3.82 ± 0.010		1.31 - 1.33
c.	0.153 ± 0.005		3.82 ± 0.010		1.33 - 1.40

Since the largest number of specimens fell into the group (b) range, this group of coupons was used throughout the investigation. Random sampling and repeated visual inspection insured that any significant "size effect" due to specimen irregularity was randomized and that spurious effects due to macroscopic surface defects were eliminated.

PICKLING AND COUPON PREPARATION

Coupons were selected in batches of eight for the reaction tests. The number was dictated by the use of four reaction vessels in which duplicate samples were run. Coupons were identified by a number, stamped into one upper corner. They were suspended in the reaction vessel by means of a glass hook running through a one-eighth inch hole drilled as shown in Fig. 9. The hole was carefully de-burred using a one-half inch drill to guarantee the absence of abnormal metal loss during the subsequent corrosion tests due to a loss of weakly adhering metal burrs.

The as-received specimens carried a heavy mill scale layer (Fig. 22). It was felt that heterogeneities present in this layer would introduce greater sample irregularity than a clean metal surface and thus a means of descaling was required.

A pickling procedure appeared to be most suitable since mechanical

preparation of a three dimensional sample, requiring close reproducibility and repeating the procedure for perhaps two hundred specimens, appeared both laborious and unnecessary. Secondly, the specimens were to be used in an acid environment in which hydrogen would be evolved, so acid pickling offered no disadvantage. Although industrial pickling is normally done in sulfuric acid solutions, the present problem was solved using the more expensive hydrochloric acid for the following reasons:

1. Neither sulfuric nor nitric acids produced a cleaner surface than hydrochloric acid,
2. To eliminate the possibility of surface contamination by sulfur compounds and
3. The system under study consisted of aqueous hydrochloric acid.

Pickling tests indicated a 50:50 solution of acid in distilled water as the best concentration. Immersion was maintained, with gentle agitation, for two and one-half minutes at 55°C; a clean metal surface resulted, requiring no further treatment.

The coupons, pickled in batches of eight, were first inspected, hung on a glass holder and then immersed in the bath. After pickling, they were immediately transferred to a cold distilled water bath. From this time on, the specimens were handled only by laboratory nickel-plated tongs. The coupons were removed from the hanger and water bath individually, given a brisk wash in the bath water, then washed and dried with acetone using a small hot air blower. The coupons were then weighed prior to use in the reaction vessel.

The time required for this operation was standardized to one-half hour from time of pickling to time of use in the reaction vessel. Although

no truly significant effect on corrosion was found due to an extended time of exposure to laboratory atmosphere, the fixed schedule was maintained to guarantee a consistent thickness of new oxide film on the fresh metal surface.

ACID CLEANING GLASSWARE

All glassware used in the investigations was first cleaned in distilled water prior to immersion in chromic acid[45]. The duration of immersion in the cleaning acid was not less than one-half hour. Glassware was then washed in cold distilled water, immersed in boiling distilled water for ten to fifteen minutes, followed by a distilled water rinse and drying (using the hot air blower).

Handling of all glassware was kept to a minimum and care was taken to maintain a clean outer surface in an effort to reduce possible contamination of solutions by skin oils and dust. The glass apparatus was assembled using rubber gloves and tongs were used when handling the small beakers and supporting rods.

SOLUTION PREPARATION

The selected pH for the entire series of tests was pH 1. Since a large number of tests were to be conducted and since four reaction vessels were available, sufficient solution was prepared for carrying out four duplicated weight-loss tests. By adjusting the specimen heights within the reaction vessels to allow complete immersion at high agitation in a solution volume of about 490 cc, a two-litre solution of inhibited acid was required for each reagent evaluation series, allowed precise solution formulations, and also obviated any difficulties created by varying the ratio of solution

volume to coupon area. The quantity of acid required for the correct pH was 21 cc. This volume was measured by pipette and checked using the pH meter.

Due to the limited solubility of the higher molecule weight alcohol and acid surfactants, solution preparation was troublesome. The difficulties were overcome by utilizing the solubilization property of the amine micelle solutions.

Aliphatic amines are readily soluble in hydrochloric acid as a result of their conversion to the readily ionized amine hydrochloride. The formation of micelles allows other non-polar or polar-non-polar molecules to be incorporated (solubilized) within the micelles.

A successful procedure was evolved using the following steps:

1. When long chain (C_{16} or C_{18}) carboxylic acids were to be evaluated, it was found necessary to reduce the coarse crystal size of the as-received material to a fine powder. If lumps remained in the powder, solubilization was unduly time consuming.
2. Each prescribed quantity of reagent was weighed in an individual pH meter beaker using the micro-balance.
3. Two or three drops of the required 21 cc. of concentrated hydrochloric acid were added to the amine only; the remaining acid transferred to a two litre volumetric flask in which the solution was to be prepared.
4. Using a clean glass rod, the amine was pulped thoroughly with the acid in the small beaker and allowed to stand for 10 to 15 minutes.

5. The remaining reagents were then transferred from their beakers into the amine hydrochloride pulp. Residual reagent adhering to the beakers was washed directly into the two litre flask with distilled water.
6. The entire reagent mixture was then pulped to a creamy consistency in the amine beaker and again allowed to stand for 10 to 15 minutes.
7. Using distilled water, the mixture was then washed into the volumetric flask until the contained volume was about 500 cc.
8. The flask and contents were heated over boiling water to 50 or 60°C and shaken vigorously. Water addition followed by vigorous mixing was repeated alternately until a volume of about 1500 to 1800 cc was prepared. At this time, careful visual observation of the solution was made to determine if any undissolved solids were present. If they were, successful solubilization by repeated heating and mixing was often attained, but frequently, further mixing proved futile and the reagents had to be prepared again. The most difficulty was encountered with the carboxylic acid constituents and only careful size reduction (as mentioned in point 1) allowed proper dissolution.
9. If no undissolved solids were present, the solution was made up to the etched mark, mixed and allowed to cool. At room temperature the final water addition was made and the solution reheated to about 50°C and remixed. The volumetric flasks were kept sealed except for frequent stopper loosening to equilibrate the internal pressure during heating and cooling periods. At a

temperature between 30 and 40°C (the Krafft Point), the colloidal solutions became clear and were then assumed to be homogeneous and ready for the weight-loss tests.

The foregoing procedures were used in the case of the solid reagents but the shorter chainlength liquid reagents, having a higher vapor pressure, were decanted and washed directly into the volumetric flask to reduce volatile losses. The liquid amines were first treated with hydrochloric acid (as in point 3 above) before being transferred to the flask.

METALLURGICAL EXAMINATION

Numerous specimens were selected in order to study the results of both inhibited and uninhibited reactions. They were cut and arranged to display the end, edge and face surfaces for microscopic examination.

The standard methods of bakelite mounting, grinding, polishing, and etching were utilized. Photomicrographs were all taken at the same magnification for comparative purposes.

SURFACE TENSION MEASUREMENTS

The apparatus, as illustrated in Fig. 6 was placed on a concrete table to limit vibration effects within the building. The syringe, used in the determinations of drop volume, was cleaned in the acid cleaning mixture prior to use for measurements. The syringe tips were polished using the standard polishing procedure for metal specimens. Preparation began on the grit emery paper, progressed to 600 grit and a final light polish was applied using magnesium oxide polishing compound. The polished tip was observed at about 150 magnification to assure that no edge defects were

present. The tip diameter was then measured by goniometer.

Solutions prepared in the manner previously described were diluted in the following way:

1. The required volume of uninhibited aqueous acid, pHl was pipetted to each 100 m.l. volumetric flask.
2. The inhibited acid solution was heated to approximately 50°C, then, having accurately observed the temperature, the required volume of solution was transferred to each volumetric flask. The flasks were kept stoppered in cold water to assure minimum volatile losses of inhibitor.
3. Each diluted solution was then heated to about 50°C, mixed, and a few m.l. poured into the apparatus reservoir. The syringe, mounted in position, was then dipped into this solution and a small volume of it taken into the syringe. By inverting the assembly and moving the plunger up and down several times, the plunger and syringe wall became wetted by the solution and in this position the last trace of air was expelled from the syringe.
4. The solution remaining in the reservoir was swirled to wet the surface and then discarded. The water jacket was connected to the apparatus and the reservoir filled with the solution to be tested. (Care was taken not to create air bubbles which were later taken into the syringe).
5. The reservoir was then quickly lowered into position, the assembly connected and the thermostatically heated water circulation started. Equilibrium was reached in about one-half to three-quarters of an hour.

Upon reaching equilibrium the syringe was loaded and discharged several times to assure that the plunger and syringe wall were wetted, thus eliminating possible drop volume error due to capillarity effects. The syringe mechanism was then locked in place and readings taken.

The initial 80 or 90% of the drop was formed rapidly but the final volume addition was made over a period of about one minute so that the whole drop took from one minute to one and one-half minutes to part after the final volume increase was made.

WEIGHT-LOSS CORROSION TESTS

The corrosion tests were carried out in 1000 m.l. flasks containing 490 cc of solution. The assembly is illustrated in Fig. 5 .

Pickling and weighing were described earlier and it was pointed out that one-half hour elapsed from start of pickling until the specimens were placed in the reaction solution.

The reaction vessels were heated electrically by a heating mantle with solution temperature manually controlled using a powerstat. Mixing speeds were also manually controlled to the desired 1,000 r.p.m. (measured by the strobotac). Both temperature and mixer speed were at the correct values and stabilized before the specimens were immersed.

Fluctuations in both cooling water pressure and line voltage necessitated frequent adjustments to both mixer speed and heater setting, but variations were held to within $\pm$ 1°C and within $\pm$ 30 r.p.m.

Initial tests of twelve hour duration, conducted to evaluate and compare the inhibitors selected, were run at 60°C. However, the results were not consistent and scatter was much larger than could be accepted. At the

same time, test-tube tests were used in an effort to derive fast data on the relative inhibition produced but results again were too badly scattered to be of any great use.

Investigations into the causes of this wide scatter included sampling, pickling, temperature control and mixing speed and indicated that adequate controls were not being taken. The correct sampling and pickling procedures, (outlined previously) mixer speed and temperature controls led finally to the acceptable results of the last test series.

The reaction time used for evaluating the various inhibitors was six hours, after which the specimens were removed, placed in distilled water, brushed vigorously (under water) with a nylon tooth brush, rewashed in water and dried with acetone using the hot air blower. The specimens were then weighed and the weight-loss determined.

All specimens were used once only. Eight tests were carried out on each inhibited solution under identical conditions of time, temperature and inhibitor and acid concentration.

The reaction rate in uninhibited HCl solution was determined by removing the specimens after a specified period of immersion (and followed by brushing, washing and drying before the weight-loss was determined). Immersion times for this test varied from a few minutes to several hours. Again, repeated measurements were made to obtain the best average weight-loss value.

Since the specimens used in determining the uninhibited weight-loss curve were being removed and returned to the solution several times during the course of a test, it was necessary to investigate the time taken for a cold specimen to reach the solution temperature. To answer this, a specimen

was equipped with an internal thermo-couple lead and connected to the oscilloscope. The cold junction was at specimen (room) temperature and the solution at 60°C. Just prior to immersion of the sample, the shutter of the Polaroid Land Camera was opened to the fluorescent screen. Upon immersion, the electron beam path on the oscilloscope screen was recorded on the film (Fig. 7).

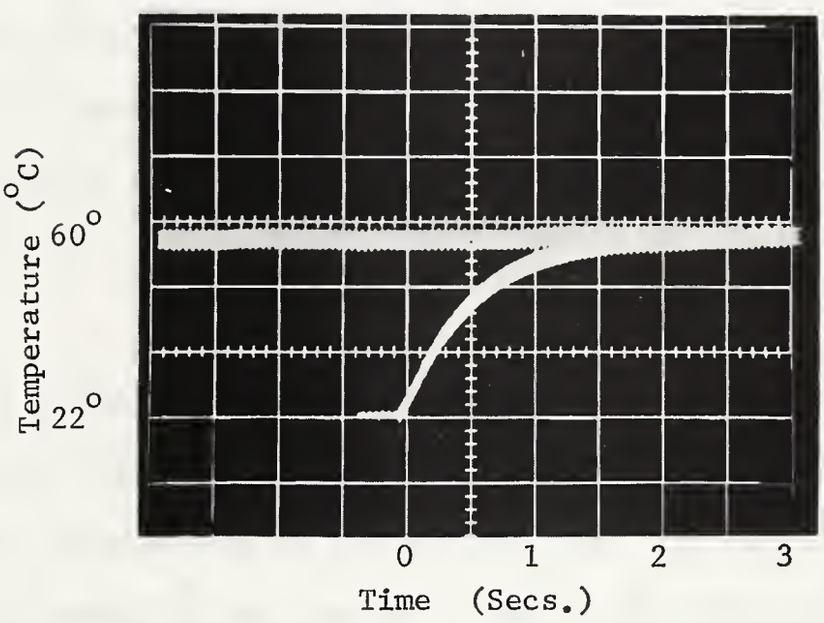

Fig. 7 Oscilloscope Trace of Coupon Heating Time

EXPERIMENTAL RESULTS

UNINHIBITED REACTION TESTS

General

Preliminary weight-loss tests were unacceptable due to the widely ranging scatter of results. This difficulty was obviated with the use of a second batch of test specimens and the subsequent study of reaction variables. Data typical of the preliminary tests are shown in Table B-1

Coupon Size

The sample size variations, as previously pointed out, provided one source of scatter. The corrosion taking place on these specimens was not general but was concentrated on the end and edge faces of the coupon (Figs. 9, 24). Since any change in the specimen width affects the relative proportion of more corrosion active sides (edges), the well known catchment area principle undoubtedly comes into effect and widely varying corrosion rates can be obtained by slight modification of the width dimension.

Temperature

Due to fluctuating power, the temperature control was not good over the initial 13 hour test period. The immersion time was reduced from the initial 13 hours to 6 hours thus allowing a more continuous visual check to be maintained. The temperature variation was thus reduced from a range of $60 \pm 5^{\circ}C$ to a range of $60 \pm 1^{\circ}C$.

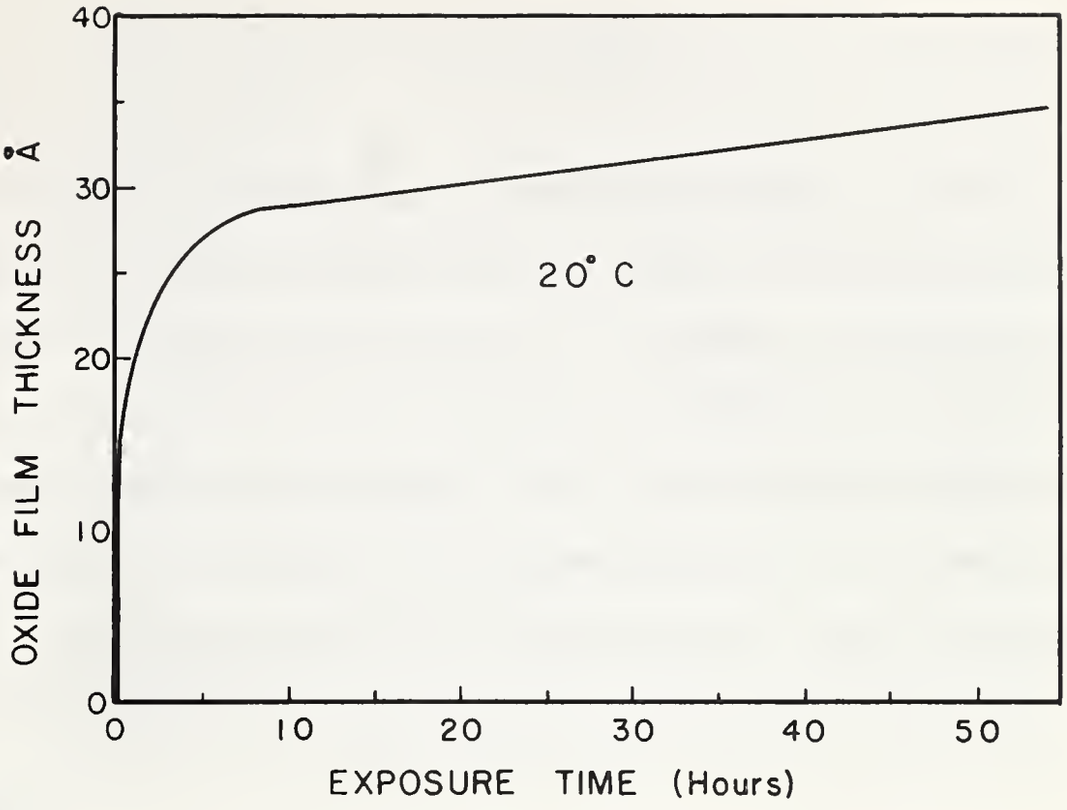

Fig. 8 Iron Oxide Film Growth

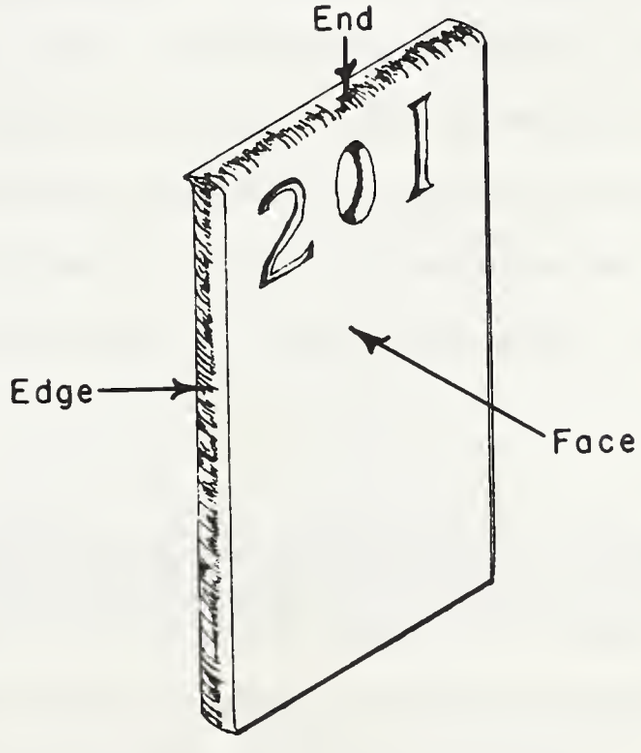

Fig. 9 Coupon Specimen

Aging Time

The elapsed time following the pickling and weighing operations, until the specimens were immersed in the reaction vessel is referred to as the aging time. During this interval the specimens are exposed to and oxidized by laboratory air. Fig. 8 relates the thickness of oxide film on clean metal at room temperature to time of exposure. Tests were conducted varying the exposure time from 1 to 3 hours in a dessicator, the results of which were inconclusive. The exposure time for all specimens was, however standardized to exactly 30 minutes.

Mixer Speed

Table B-2 shows the variation of weight-loss with mixer speed for 6 hour immersion tests at 60 $\pm$ 1^{o}C. The apparent difference between the high corrosion rate with high agitation and lower rate with low agitation is shown to be real. A Students' Test of Significance (Appendix B) indicates the confidence limit to be between 99 and 99.9%, while an analysis of the variance in the two sets of weight-loss data indicates that the two sets of samples come from the same population, i.e. that they are comparable. As a result, subsequent weight-loss tests were all conducted at 1,000 r.p.m.

Grain Structure

Microscopic observation of the as-received lot 1 coupons indicated clearly a very large grain size gradient through the coupon (Fig. 10) This suggests that the final rolling treatment was done at a sufficiently high temperature to cause grain growth at the outer surfaces.

The end and edge grain structure was drastically deformed due to shearing. The internal structure, unaffected by either the last rolling step or

x80

Fig. I0 Edge View of As-Received Lot No. I Coupon

x80

Fig. II Edge View of Lot No. I Coupon Annealed in Argon I.3 Hours at 820° C

the shearing, did show, however, small grain boundary regions of carbides, and included sulfides and distinct phosphorous "ghosts".

An attempt was made to eliminate the deformed metal through annealing (Fig. 11) in an argon atmosphere for 80 minutes at 1480°F. The result did, in fact, eliminate this material which recrystalized at the outer levels but extensive grain growth also took place at the region of 10 - 15% cold work. Although the corrosion rate was reduced in these specimens from 2.7% weight-loss to 1.5%, the problem of controlled argon annealing was troublesome. This problem was obviated by the use of a second lot of specimens which displayed a much smaller grain size gradient and smaller shearing effect. This is demonstrated by the extreme grain growth observed in coupons of lot 1 compared to the last lot (Figs. 11 and 26).

The corrosion tests of the second lot provided much more acceptable data. Scatter was still evident but the results of the 6 hour, 60°C tests, (Table B-3) show clearly that the scatter had been reduced by the change in the structure and by the close controls maintained. The resultant frequency distribution of weight-loss data (Fig. 27) bears this fact out.

Time-Temperature Studies

In order to provide complete information for inhibitor evaluation, and to determine what was the possible controlling feature of the uninhibited reaction (through the determination of an experimental activation energy), a number of weight-loss studies were carried out at 60, 80, 90 and 95°C. These results are shown in Figs. 12, 13 andTables C-1, C-2, C-3 and C-4.

The significant point of interest is the shape of the curves. What might be considered as a double discontinuity is clearly evident in all cases,

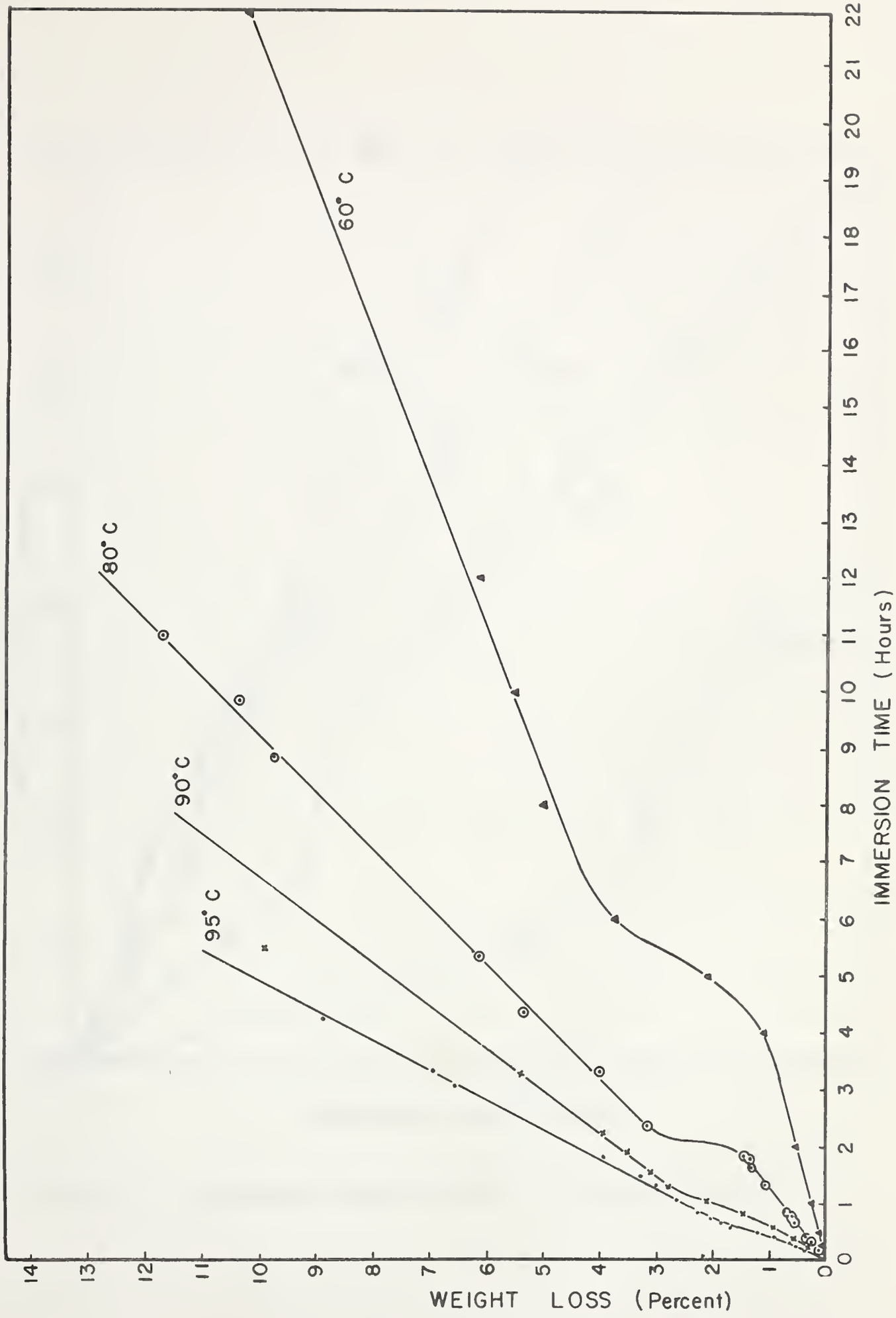

Fig. I2 Uninhibited Weight-Loss Data - Pickled Specimens

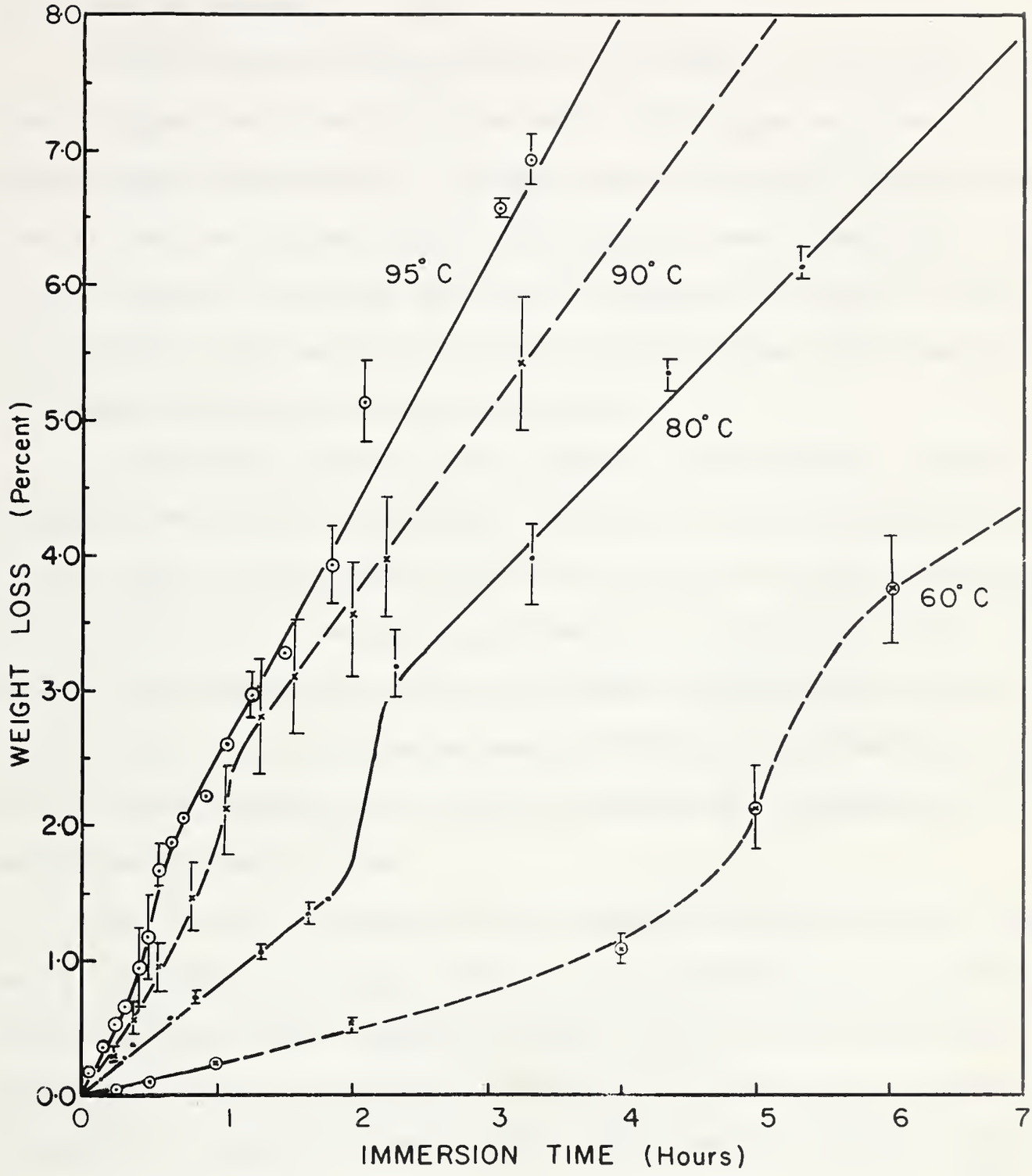

Fig. I3 Uninhibited Weight-Loss Data - Pickled Specimens

with an additional discontinuity appearing in the 90° curve (Fig. 14) of the unpickled specimen.

On the expanded time-weight-loss scale of Fig. 13, the curves can be seen to appear continuous and not to suffer sharp breaks as in the other almost linear representations. In fact, there is only one linear portion, that is the final portion of the curve beyond the last discontinuity. Of further interest is the fact that in all but one of the family of curves the corrosion rate does not level off or become constant until from 2½ to 3½ weight percent of the metal is dissolved.

The exception to this is the corrosion of the unpickled specimens studied at 90°C (Fig. 14, Table D). In this case, the first reaction involves largely the dissolution of the mill scale and then metal dissolution. This feature adds yet another discontinuity to the weight-loss curve. If, however, the weight-loss is calculated between the first and last discontinuity, it is found to be approximately 2½ weight percent therefore supporting the former observation of constant corrosion rate following 2½ to 3½ weight percent loss of metal.

The uninhibited reaction, strongly directed through the end and edge metal, is illustrated in Figs. 24 and 25. It is accompanied by a rapid hydrogen evolution which accelerated greatly at the elevated temperatures. A detectable quantity of hydrogen sulfide was also generated, as well as an insoluble - or rather, a slowly soluble, black, reaction product. The reaction product, clearly evident when brushing the samples from the 60°C study was, however, absent in the 80, 90 and 95°C studies. Presumably, its solubility is increased at the higher temperatures and it may also be stripped from the surface by the violent evolution of hydrogen.

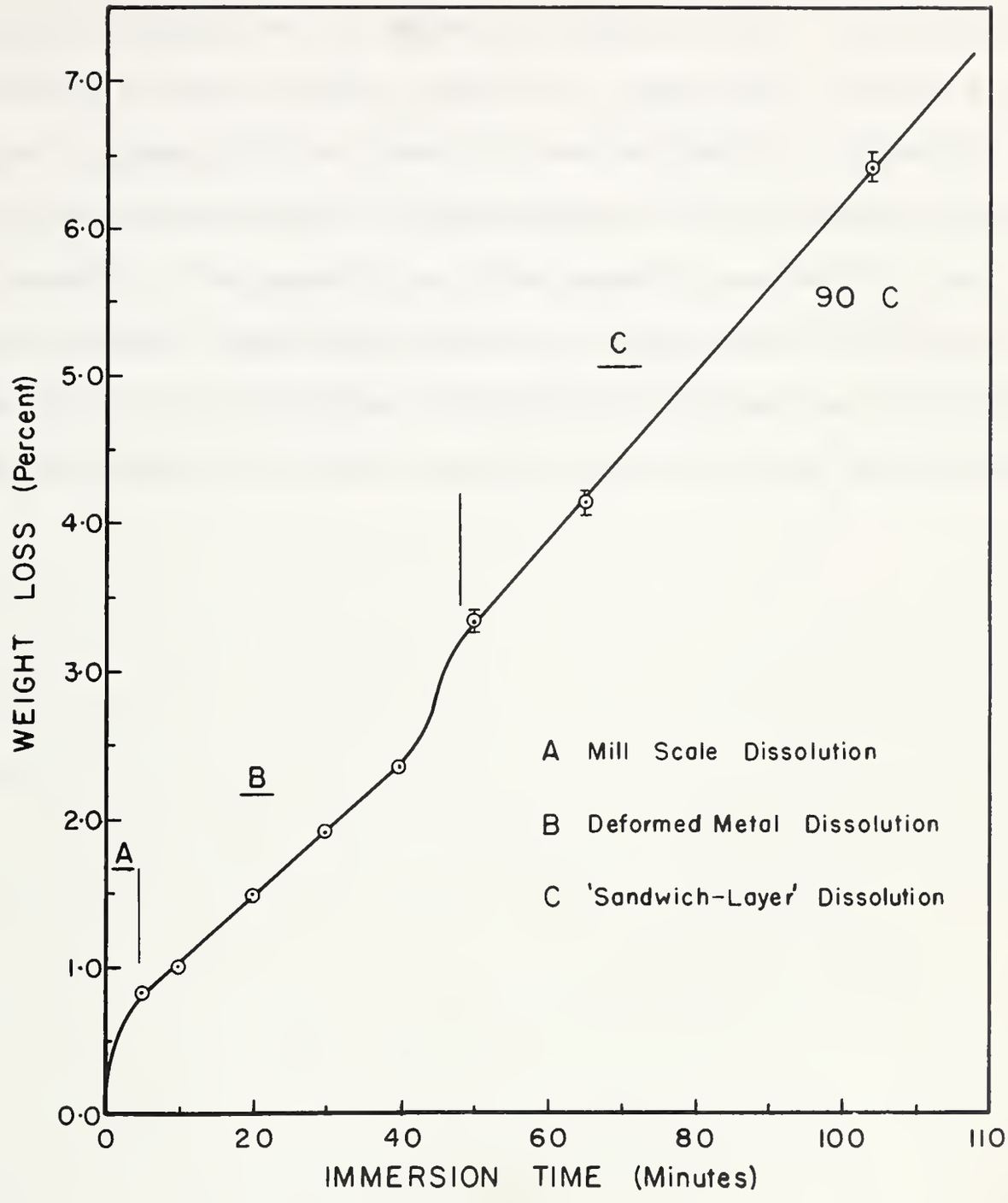

Fig. I4 Uninhibited Weight-Loss - Specimens not Pickled

Reproducibility was very good in these investigations with the exception of the data for the uninhibited reaction of 95°. Additional observations to ensure constant temperature, mixing speed, specimen size and surface appearance did not produce the desired control. The boiling point of the solution was found to be approximately 97°C and in fact, boiling was observed in the general area of the magentic mixer while it was in operation and this feature was believed to be the cause of the inconsistent results. Fig. 13 illustrates the variation in the data and the plotted line is judged to be the best average, based on the other data presented.

INHIBITED REACTION TESTS

General

The first object of these tests was to evaluate the numerous reagents on hand beginning with determining the characteristics of the amines. As pointed out earlier, successful dissolution of the carboxylic acids proved difficult in the preliminary tests, so the short chain molecules were not considered and the evaluation of the remaining homologs was carried out in combination with selected amines. The same was true for the longer chain alcohols and in an effort to limit experimentation due to the limited number of specimens on hand, these too were used in combination.

The initial tests were all carried out at 60°C using an immersion time of 6 hours. Later tests showed the effect of time, temperature and inhibitor concentration on inhibition.

The results are reported as weight-loss percent and as percent inhibition, the latter is calculated as follows:

W_1 = weight loss % uninhibited specimens at T_1 and with 6 hour immersion

W_2 = weight loss % inhibited specimens at T_1 and with 6 hour immersion

$$\% \text{ inhibition} = \frac{(W_1 - W_2)(100)}{W_1}$$

Because of the relative insensitivity of the latter figure, the plot of results is made using weight-loss % data. The above is included to

facilitate comparison of these data with those of other investigators.

Amine Evaluation

Fig. 15 and Appendix F-1 show the effectiveness of 10^{-4} molar concentration of the amine inhibitors at 60°C. The weight-loss data were all taken from 6 hour immersion tests.

The effect of increased hydrocarbon chain length is clearly evident and a comparison can be made between mono- and di alkyl amines of equivalent molecular weight. The mono-alkyl amines are significantly more effective.

Significant too, is the apparent levelling off in the beneficial effects on increasing the hydrocarbon chain. It is quite clear that the increased inhibition produced by going from C_{14} to C_{16} and C_{18} does not continue at the same rate as that of the earlier observations using amines.

The generation of hydrogen sulfide observed in the uninhibited reactions was also observed in the initial, short chain, amine evaluation tests. The evolution commenced at, or shortly after, immersion and continued throughout the 6 hour test. This was not true in tests of hexadecyl and octadecyl amine in which no hydrogen sulfide was detected at any time. Correspondingly, no hydrogen evolution was observed in tests of either of these amine inhibitors.

Since there was no clear-cut advantage in the use of the longer, octadecylamine, in all subsequent tests, only the hexadeclyamine was used.

The physical appearance of the corroded specimen quite naturally improved as inhibition improved. The high weight-loss continued to be concentrated in the deformed edge and end metal with considerable dissolution in the form of pits on the facial surface. As inhibition improved, however,

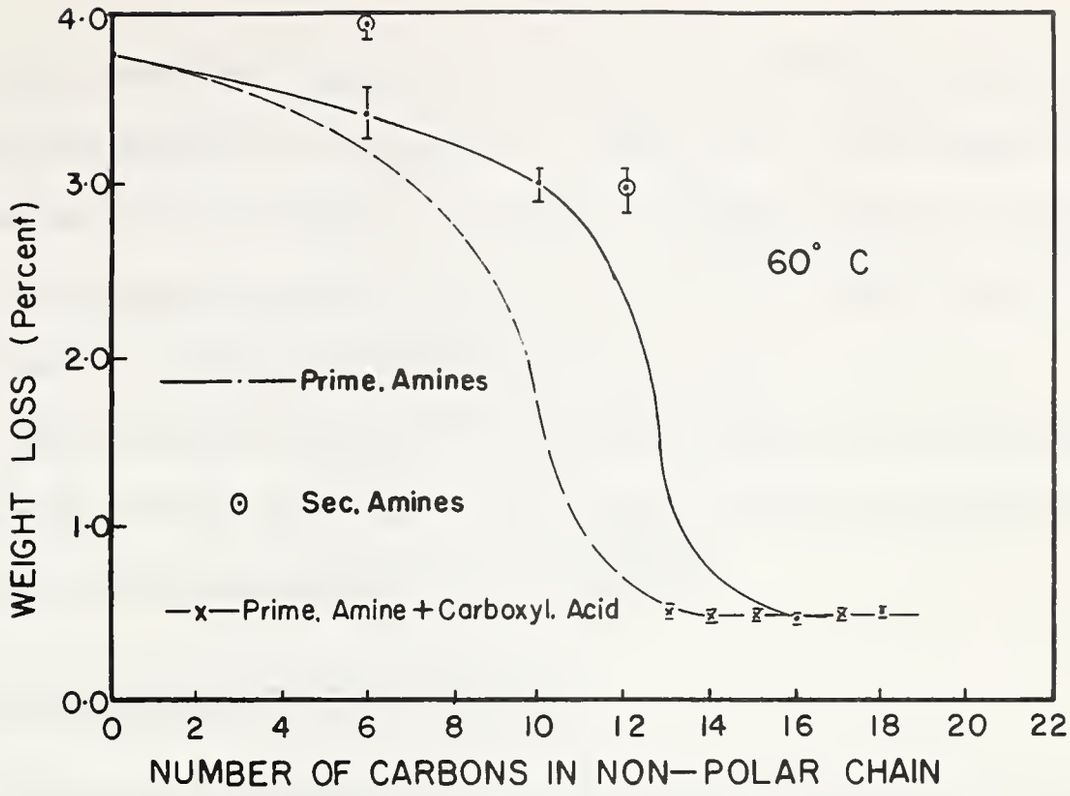

Fig. I5 Effect of Non-Polar Chain Length on Inhibition

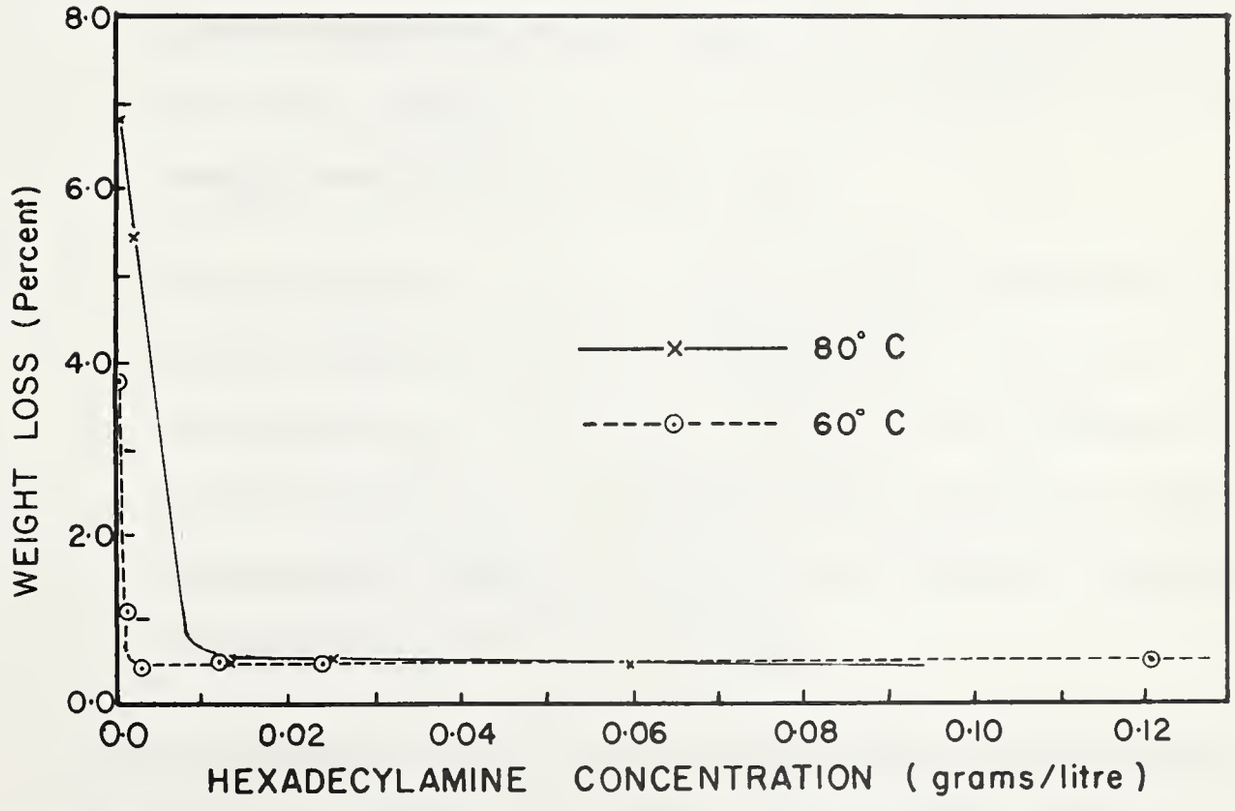

Fig. I6 Critical Inhibitor Concentration

the facial corrosion disappeared, leaving the localized penetration through the deformed regions as the source of metal loss. With hexadecyl and octodecylamines, the face surface was bright, although somewhat dulled by the film. The deformed regions were almost intact but widely spaced and apparently very deep localized pitting had taken place.

The specimens inhibited with hexadecylamine were clearly hydrophobic to the acid reaction solution. This feature was not eliminated by the cleaning process following removal of the specimen.

Critical Concentration for Inhibition

The effect of hexadecylamine (C_{16} amine) concentration on inhibition is shown in Fig. 16 and Table F-2. The tests were carried out at both 60 and 80°C. The two resultant points of interest are these:

1. Maximum inhibition does not appear to be temperature sensitive with this surfactant since, at both 60° and 80°C, the minimum weight-loss was approximately 0.05%.

2. There appears to be a very definite minimum concentration below which inferior inhibition is encountered. A significant effect of temperature is noted here. A rise of twenty degrees from 60° to 80°C increases the minimum effective concentration from approximately 0.001 gms/litre (0.4×10^{-5} molar) to approximately 0.01 gms/litre (0.4×10^{-4} molar).

Metal dissolution in this series of tests was identical to the above description with the exception that the protective nature of the film breaks down very suddenly, as illustrated, and as a result, no gradual

degradation was observed. The break point is sharp, the resultant dissolution rapid, and the concentration could mark the minimum requirement for a monomolecular amine film coverage.

Evaluation of Surfactant Combinations

This series of tests was adopted for the purpose of comparing the various inhibitors both from the standpoint of the active functional groups involved and the length of the hydrocarbon chains.

The first comparisons involved the carboxylic acids in combination with the hexadecylamine and are shown in Fig. 17 and Table F-3. The immediate conclusion is that there was no apparent synergistic effect and added variation of the length of hydrocarbon chain had no truly significant effect on the inhibitive property of the combination. The macroscopic appearance of the specimens after immersion varied little from specimens inhibited with amine only, and the weight-loss was again localized in scattered, deep pits in the regions of deformed metal.

Since equivalent total molar concentrations of surfactants were used, under identical test conditions throughout this test series, direct comparisons between inhibitor combinations are possible.

The addition of the third (alcohol) component affected the nature of the film and resulted in increased inhibition (Fig. 17, Table F-4). However, increased hydrocarbon chain lengths of the components had a deleterious effect, as observed earlier by Hackerman[16]. (This is explained in a later paragraph, page 70).

The improvement was not sufficient to eliminate the deep pitting nor was it, in fact, discernible on macroscopic examination.

The addition of a fourth component, sodium dodecyl sulfate, did have a dramatic effect on the inhibitive properties of the combined reagents.

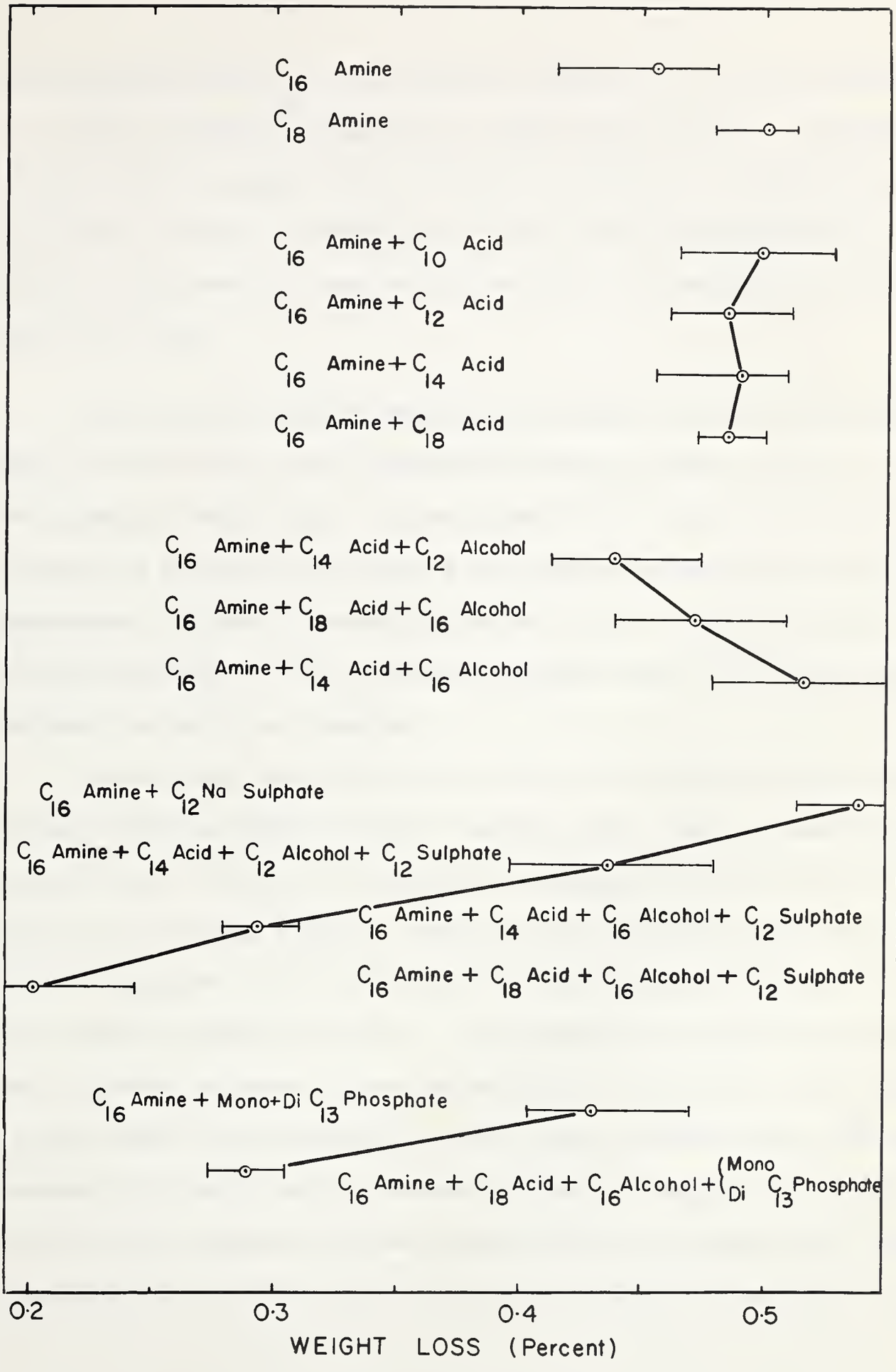
C16 Amine
C18 Amine
C16 Amine + C10 Acid
C16 Amine + C12 Acid
C16 Amine + C14 Acid
C16 Amine + C18 Acid
C16 Amine + C14 Acid + C12 Alcohol
C16 Amine + C18 Acid + C16 Alcohol
C16 Amine + C14 Acid + C16 Alcohol
C16 Amine + C12 Na Sulphate
C16 Amine + C14 Acid + C12 Alcohol + C12 Sulphate
C16 Amine + C14 Acid + C16 Alcohol + C12 Sulphate
C16 Amine + C18 Acid + C16 Alcohol + C12 Sulphate
C16 Amine + Mono+Di C13 Phosphate
C16 Amine + C18 Acid + C16 Alcohol + (Mono Di C13 Phosphate
SINGLE AND MULTI—COMPONENT INHIBITORS
0·2
0·3
0·4
0·5
WEIGHT LOSS (Percent)

Fig. 17 Multicomponent Inhibition

As illustrated in Fig. 17 and recorded in Table F-5, the initial addition of the sulfate to hexadecylamine did not improve the inhibition. Subsequent addition of the carboxylic acid and alcohol to form a four component inhibitor clearly increased the effect and further, by increasing the chain length of first the alcohol and then the acid molecule, the weight-loss was reduced from 0.5 to 0.2%.

The effect was clearly observed. The edge and end pits were eliminated, the burrs left after pickling were clearly evident and only a slight and apparently overall metal loss was discernible on the deformed structure. The metal in the small hole (drilled for purposes of suspension) showed no degredation, the metal remaining bright and shiny. Even at the point of the possible concentration cell where the specimen rested on the glass support, the metal was bright and unmarked.

In all cases, the hydrophobic nature of the adsorbed film was clearly evident before and after the final cleaning process which followed the immersion tests. The film was essentially transparent in the case of the single, two and three component inhibition, although dull areas on the surface were apparent. The film was quite easily observed in the case of the four component sulfate inhibitor. The specimens were "thick" to the touch and slippery in addition to being hydrophobic. The film was often colored a slight yellow and occassionally, short, thick appendages were observed - presumably film which had been damaged and was dislodged from the surface. The thick multicomponent film was removed from the specimen by the final cleaning process but the surface continued to display a hydrophobic nature.

TIME AND TEMPERATURE EFFECTS ON INHIBITED CORROSION

The excellent performance of the multicomponent film at 60°C led to a test of this combination at 80°C. The results (Fig. 18-C, Table F-7) showed a large sensitivity to temperature which resulted in a drastically reduced inhibitive effect.

Since the hexadecylamine alone had displayed very good inhibitive properties at this temperature, the proportion of this component was increased and the sulfate replaced by a commercial phosphate (a 50:50 mixture of mono and di-tridecyl orthophosphate). The resultant inhibition (Fig. 19-D, Table F-8) proved promising and additional tests over extended immersion times showed that inhibition was improved.

This combination was also studied at 60°C (Fig. 19-E) but was found to be inferior to the four component sulfate, which displayed a very good stability over longer immersion test periods.

The four component phosphate displayed again a multilayer film which was removed in the final cleaning process but left a residual, invisible, hydrophobic film. Unlike the four compenent sulfate, however, its attachment at 80°C appeared to be much firmer and the resistance offered to hydrogen evolution was marked by the formation of very large hydrogen bubbles. The fluid flow past the specimens had a very decided effect on the removal of these multilayers from the surface as did the evolution of hydrogen, for once the film was disrupted, hydrogen evolution was very rapid.

The order was, however, reversed at 60°C. The four component phosphate inhibitor was decidedly inferior to the one containing sulfate and displayed film breakdown very similar to that of the sulphate at the higher temperatures. That is, film stability was inferior on the edge surface leading

Figure 18 Captions

a. Uninhibited Reaction $80^{o}C$

b. Uninhibited Reaction $60^{o}C$

c. Four component (equimolar) inhibitor $80^{o}C$

C_{16} amine, C_{16} alcohol, C_{18} acid, C_{12} sulfate

d. Four component (equimolar) inhibition $60^{o}C$

C_{16} amine, C_{16} alcohol, C_{18} acid mono + di C_{13} phosphate

e. Four component (equimolar-phosphate) $60^{o}C$

f. Four component (equimolar-sulfate) inhibitor $60^{o}C$

NOTE: Total inhibitor concentration in all cases 1×10^{-4} molar.

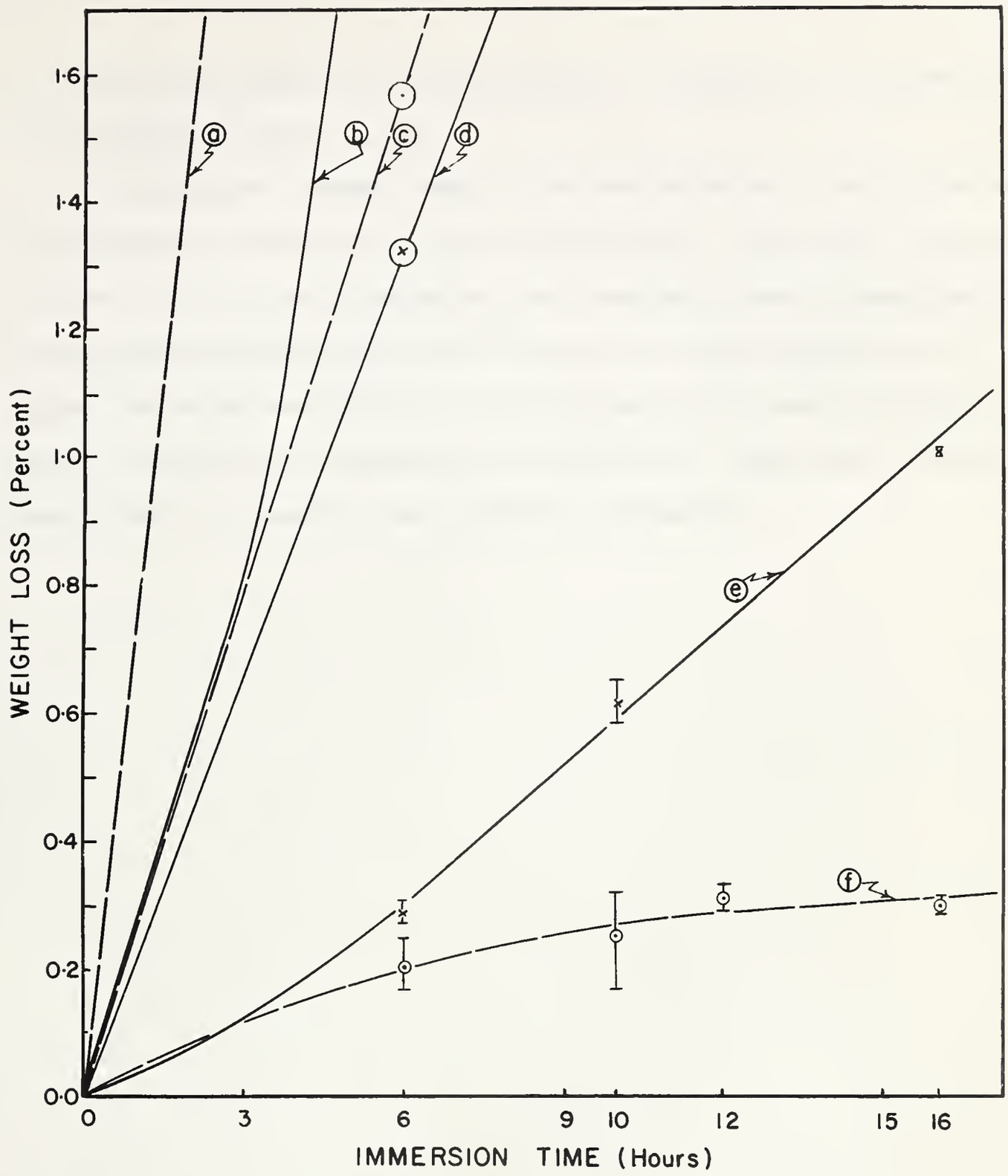

Fig. I8 Inhibitor Film Life - Time and Temperature Effects

to drastic attack where the film was removed. A comparison of the two inhibitors is shown in Fig. 19 c, d.

A significant feature common to the best inhibitor at both 60 and 80°C is the apparent levelling-off of the corrosion rate. This feature (Figs. 18-f, 19-d and 19-f) is clearly desirable since rapid metal loss is terminated after some period of reaction and a steady loss rate is then encountered, but a danger lies in the possibility of pitting rather than a general overall corrosion. In any case, an extension of the procedure, using other surfactants might reduce this hazard in any industrial application.

Figure 19 Captions

a Four component (equimolar) inhibitor — 80°C

C_{16} Amine, C_{16} Alcohol, C_{18} Acid, C_{12} Sulfate

b Four component (equimolar) inhibitor — 80°C

C_{16} Amine, C_{16} Alcohol, C_{18} Acid, C_{13} Phosphate

c Four component inhibitor — 80°C

0.5×10^{-4} M { C_{16} Amine

0.5×10^{-4} M { C_{16} Alcohol; C_{18} Acid; C_{12} Sulfate

d Four component inhibitor — 80°C

0.5×10^{-4} M { C_{16} Amine

0.5×10^{-4} M { C_{16} Alcohol; C_{18} Acid; C_{13} Phosphate

e Four component inhibitor — 60°C

0.5×10^{-4} M { C_{16} Amine

0.5×10^{-4} M { C_{16} Alcohol; C_{18} Acid; C_{13} Phosphate

f Four component (equimolar) inhibitor — 60°C

C_{16} Amine, C_{16} Alcohol, C_{18} Acid, C_{12} Sulfate

NOTE: Total inhibitor concentration in all cases 1×10^{-4} molar.

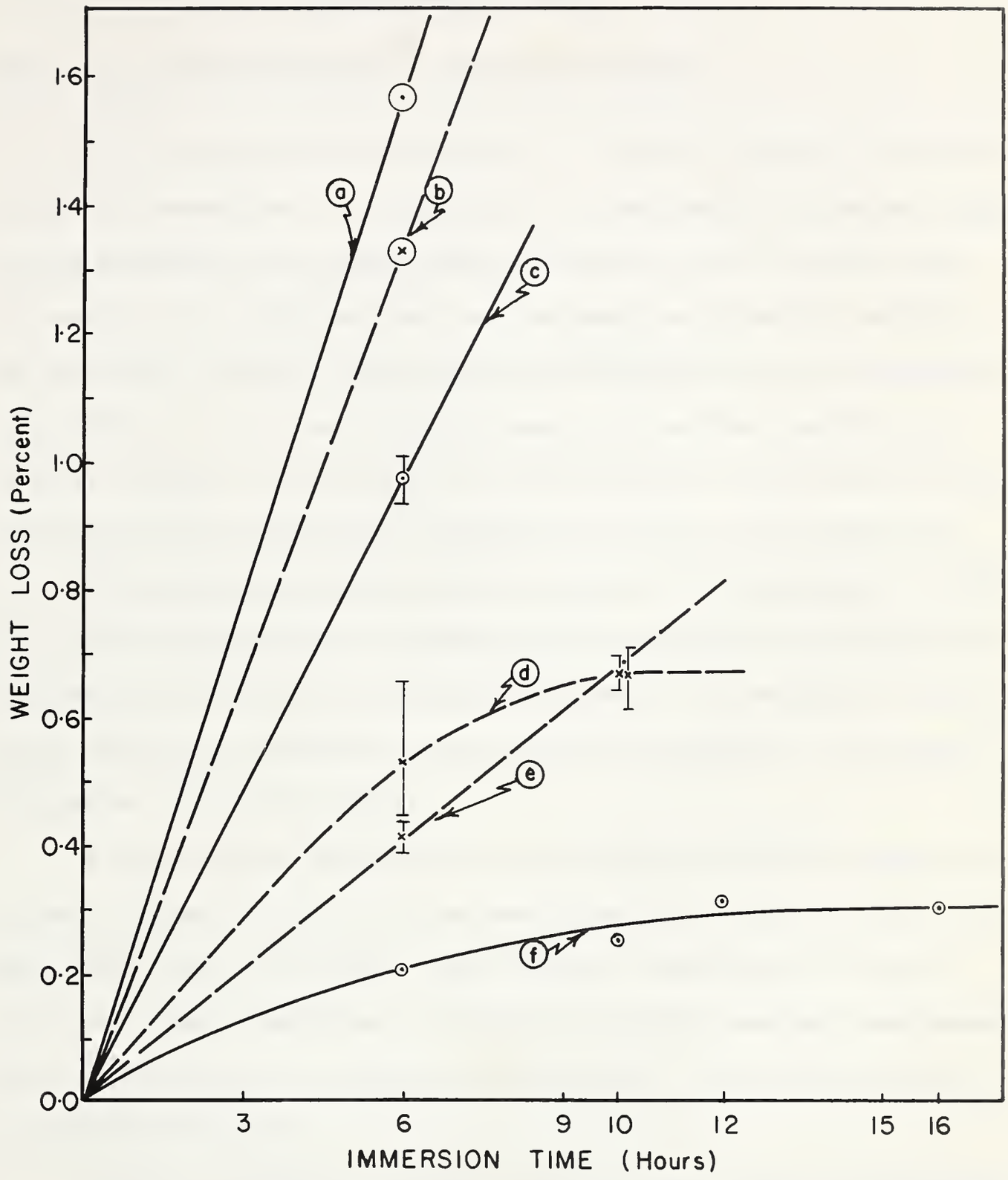

Fig. 19 Inhibitor Film Life - Time, Temperature and Composition Effects

MISCELLANEOUS STUDIES

EXPERIMENTAL ACTIVATION ENERGY - UNINHIBITED REACTION

Since the observations of uninhibited reaction rates have been made at several temperatures, an estimation of the experimental activation energy of iron dissolution can be made using an Arrhenius plot of the rate data. The results of the inhibited tests are too meagre to allow this analysis and the rather arbitrary nature of the initial portions of the uninhibited curves (Figs. 12, 13) also eliminates these portions from consideration. However, the upper, linear portions of the uninhibited rate curves are well defined and these portions were subjected to the rate study (Appendix G).

The resultant activation energy was found to be approximately 13,000 cals./mole of dissolved iron, assuming that the reaction involved only the dissolution of iron with the evolution of hydrogen. The magnitude of this energy leads one to believe that the controlling mechanism is the chemical combination of reacting species.

A rough estimate showed that the experimental activation energy for the multicomponent-sulfate inhibited system was of the order of 1,000 cals./mole. This value is of interest only in that it approaches the value of activation energies exhibited by diffusion controlled reactions (approximately 3,000 cals./mole) and is indicative of the probable controlling process in the inhibited reaction.

It must be remembered, however, that the above values for experimental activation energies are calculated from rather meager experimental results and serve an illustrative purpose only.

MONOMOLECULAR FILMS

The plot of weight-loss v.s. inhibitor concentration (Fig. 16) suggests the possibility of a critical inhibitor concentration for the formation of a monomolecular film.

Inhibitor Required for Mono-layer Film

Coupon Surface Area (from caliper measurements)

$$= 3.82 \times 1.32 \times 2 = 10.10$$

$$3.82 \times 0.153 \times 2 = 1.17$$

$$1.32 \times 0.153 \times 2 = 0.40$$

$$11.67 \text{ cm}^2$$

Total Coupon Surface (2 specimens) $= 23.34 \text{ cm}^2 = 23.34 \times 10^{16} \text{ Å}^2$

Amine molecule cross-sectional area = 21 Å^2

Number of amine molecules required for mono-layer

$$= \frac{23.34}{21} \times 10^{16} = 1.11 \times 10^{16} \text{ molecules}$$

Inhibitor Present in Bulk Reaction Solution

Critical Concentration (approximation) 0.001 gms./litre

This figure is based on the assumption that no loss of amine occurs in the transfer and solution preparation procedures.

Inhibitor initially present in 2 litres solution = 0.002 gms.

$$= \frac{0.002}{241} \times 6.02 \times 10^{23} = 5 \times 10^{18} \text{ molecules}$$

Inhibitor Loss Through Adsorption of Glassware

1. Surface area - volumetric flask (7" diameter, 10" neck)

$$= (3.5^2)\ (12.57) = 154$$

$$2\left(\frac{22}{7}\right)\ \tfrac{1}{2}\ (10) = \frac{31}{184}\ \text{in}^2$$

$$= 1156\ \text{cm}^2 = 11.6 \times 10^{18}\ \text{Å}^2$$

Number of amine molecules required for monolayer

$$= 11.6 \times 10^{18} = 5.5 \times 10^{17}\ \text{molecules}$$

2. Surface area - reaction vessel (6" diameter)

$$= (3)^2\ (12.57) = 114.6\ \text{in}^2$$

$$= 739\ \text{cm}^2 = 7.39 \times 10^{18}\ \text{Å}^2$$

Number of amine molecules required for monolayer

$$= \frac{7.39 \times 10^{18}}{21} = 3.5 \times 10^{17}\ \text{molecules}$$

Estimated amine content of 2 litre bulk solution

$$= 50 \times 10^{17} - 6 \times 10^{17} = 44 \times 10^{17}\ \text{molecules}$$

Estimated amine content of 500 cc reaction solution

$$= \frac{44}{4} \times 10^{17} - 3.5 \times 10^{17} = 7.5 \times 10^{17}\ \text{molecules}$$

$$\text{Number of possible monolayers} = \frac{7.5 \times 10^{17}}{0.1 \times 10^{17}} = \underline{\underline{75}}$$

The existence of a monomolecular film has not been verified. However, the above calculation has been based on the measured coupon surface area which, at best, is a very rough estimate. Figs. 23 and 25 illustrate that this estimate can be too small by a considerable degree. Consideration must also be given to the formation of metal ion-amine precipitate which will account for some consumption of surfactant and which may also form an integral part of the inhibitor film.

STATIC WATER DROP INDICATOR TESTS

The potassium ferricyanide indicator test is often used in laboratory demonstrations to locate anodic and cathodic surface regions and as a practical test to point out failure of galvanized coatings. This test was used to study the distribution and size of the anodic and cathodic regions of the metal coupons.

The indicator solution consisted of a 10% NaCl solution to which a few drops of phenolphthalein and potassium ferricyanide were added. Sufficient solution was transferred to the coupon to cover the facial surface. The reactions taking place are summarized below:

1. Anode - oxidation

   (a) $Fe^{o} \longrightarrow Fe^{++} + 2e^{-}$

2. Cathode - reduction

   (a) $2H_2O + O_2 + 4e^{-} \longrightarrow 4\ OH^{-}$

The production of the Ferrous ions at the anode induces a color change in the potassium ferricyanide as it changes from $K_3Fe(CN)_6$ to $Fe_3\left[Fe(CN)_6\right]_2$ and the color change is from a straw color to a deep blue.

The production of hydroxyl ions at the cathode also changes the normally colorless phenolphthalein solution to red. The two electrode regions are thus distinctively colored; blue at the anode and red at the cathode.

The test is necessarily short due to the ultimate formation of the oxygen concentration cell but clear indications are evident within a few minutes and reaction can be accelerated by the use of hot indicators, although evaporation then becomes high.

The results verified the existence of a few isolated anodic regions within a generally cathodic facial surface. In one instance, thirty small anodic points became visible within an estimated 3.6 cm^2 area (about 3/4 of the total facial area). At other times the anodic regions represented small areas rather than point locations.

Tests conducted on inhibited specimens were very slow to develop, the delay being attributed to the existence of an adsorbed film which survived the final cleaning procedures. The contact angle of the solution on these coupons was also noticeably larger than in the case of uninhibited coupons again verifying the existence of a hydrophobic surface due to the inhibitor film.

SURFACE TENSION DETERMINATIONS

Surface tension measurements using the drop volume technique were conducted to determine the possibility of evaluating the actual adsorption from solution of the inhibitor, from changes in surface tension of the corroding medium. The primary objective was abandoned because of the complexity of the system. Surface tension changes in the system can be created by the addition of ferrous ions and the coincident loss of hydrogen and further by the dis-

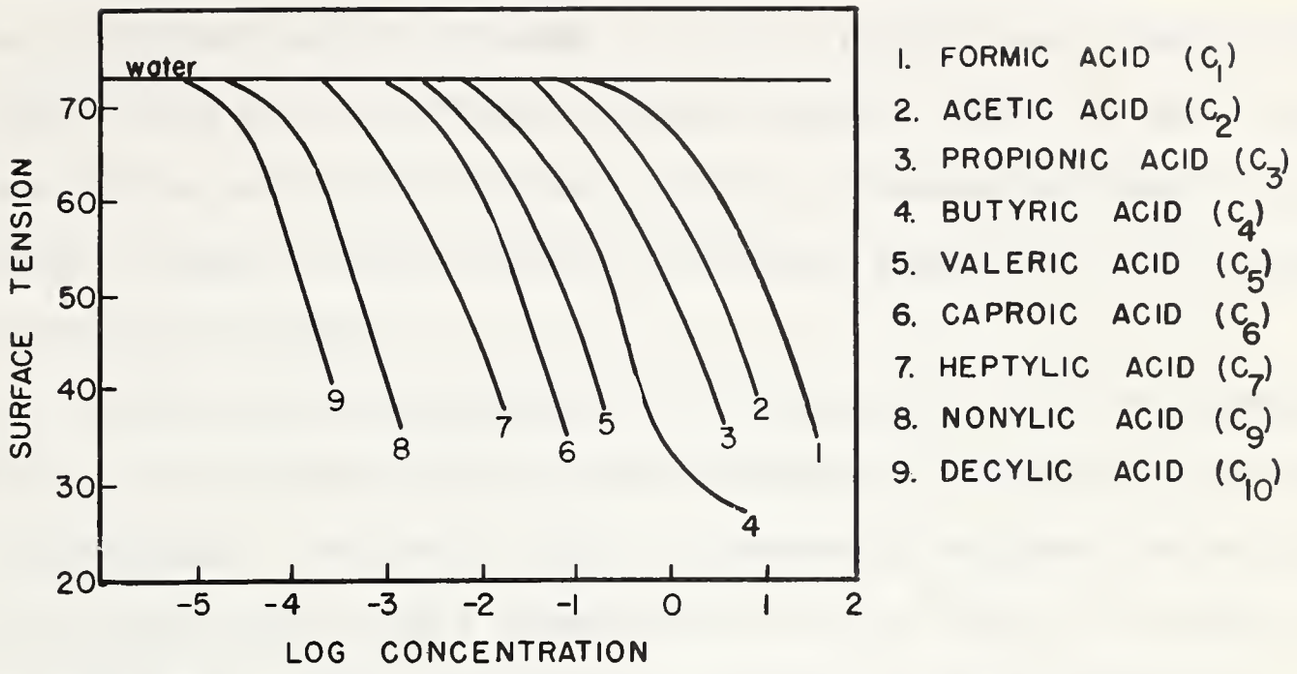

Fig. 20 Surface Tension of Homologous Carboxylic Acid Series

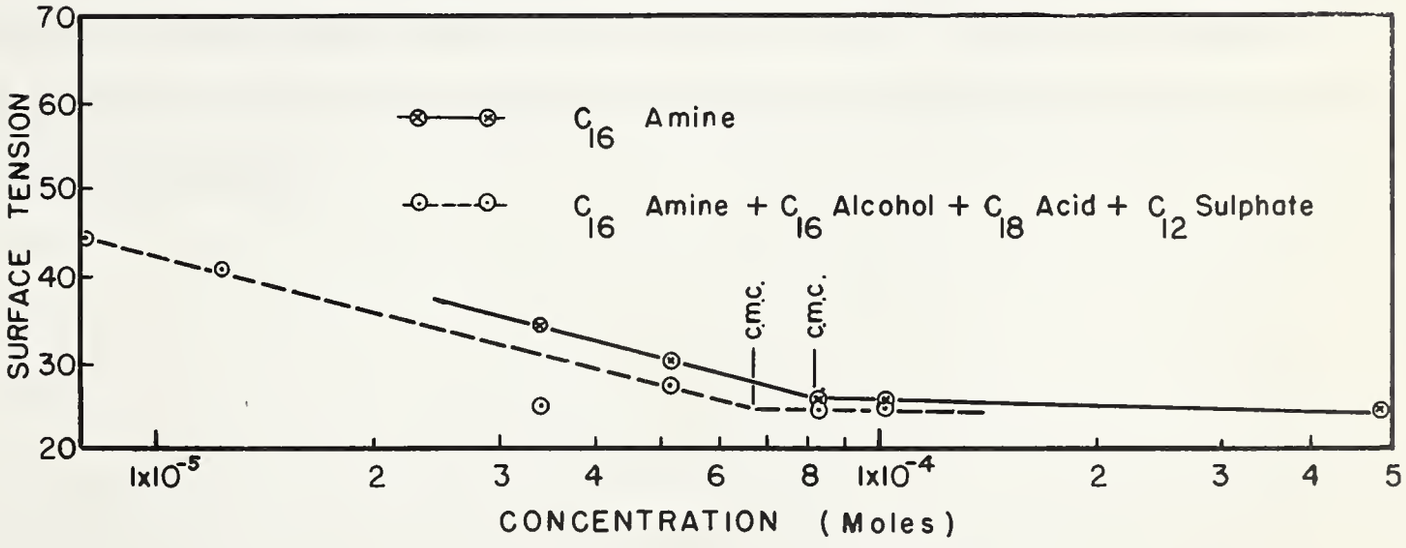

Fig. 21 Critical Micelle Concentrations, 60 C, Amine and Multicompoment Inhibitors

solution of other reaction products such as H_2S. An analytical procedure for each constituent would be necessary in order to interpret any change in surface tension due to loss of surfactant through adsorption. Also, the small surface area involved and therefore the small inhibitor concentration change, would not produce a change in surface tension of sufficient magnitude to allow accurate calculations to be made.

Surface tension measurements were carried out to verify the existence of micelles in the reaction solution and to determine the critical micelle concentration (C.M.C.). The results (Fig. 21, Appendix H) indicated that the C.M.C. of C_{16} Amine at 60°C in pH 1 aqueous HCl is 0.8×10^{-4} molar. The C.M.C. of the equimolar C_{16} Amine, C_{16} Alcohol, C_{18} Acid, C_{12} Sulfate inhibitor is 0.65×10^{-4} molar. The surface tension of the amine inhibitor at the C.M.C. is depressed an insignificant amount by the addition of the other surfactants, however, there is a depressing effect to a lower concentration range.

The existence of micelles in the inhibited solutions is thus verified, since the concentration used in all cases was 1×10^{-4} molar. Although the Krafft Point has not been accurately determined, it has been observed to lie between 30 and 40°C.

DISCUSSION

GENERAL

A small amount of information is available regarding combined reagents as inhibitors [16,27,28] but this present study is the first to employ adsorption from aqueous solutions to evaluate multicomponent inhibition.

The results support the main points of the Barrier Film Theory of inhibition.

THE UNINHIBITED REACTION

The handling of data from these and the subsequent inhibited corrosion tests was based on the fact that the data shown in Fig. 27 followed a normal distribution. This feature was useful in that it provided justification for the use of averaged weight-loss values for comparative purposes. This operation is not as dangerous as it might first seem since the scatter in the results was in a large part influenced by the amount of corrosion. The scatter range was very small (Figs. 18,19) in the case of inhibited specimens and the weight-loss differences between the various inhibitors relatively large. The main reason for the residual scatter lies in the small coupon surface areas not offering identical distributions of active sites. As a result, high temperature and long immersion tests tend to amplify this difference by a direct effect on the weight-loss encountered.

The use of the second lot of specimens provided acceptable data, as discussed in Experimental Results. Their more uniform grain structure provided a less sensitive corroding surface and thus the disadvantage of a

small heterogeneous coupon surface area was reduced.

The effect of annealing was to eliminate the metal deformed by shear and allow recrystallization to take place in these regions. If effect, the specimen then became encircled completely by a zone of recrystallized, equi-axial crystals offering a relatively uniform surface activity to the corrodant. The resulting weight-loss tests attest to the drastic lowering of the corrosion rate. However, the existence of an underlying layer of much larger grains offers a more cathodic potential to the overlying small grains and thus, as the dissolution of the fine grains is nearing completion, the "catchment area principle" can come into play, resulting in the acceleration of the corrosion rate. Since this is, in fact, an equally inhomogeneous system, the annealling procedure was discontinued.

A calculation of the estimated volume of the shear deformed metal is shown in Appendix E. Although there is uncertainty both in this estimate and in the estimated shape of the uninhibited reaction curves, it is significant that the calculated weight percent of deformed metal (3.0%) and that estimated from the curves (2½ to 3½%), coincide. The observations that reaction curves are continuous and that initial metal losses are limited largely to the end and edge surfaces, support the conclusion that deformed metal dissolution is the first stage of the coupon reactions.

Once the deformed metal has been elininated, a continuous penetration of the edge and end surfaces through the sandwich fine-grain structure results.

THE UNINHIBITED REACTION RATES

The influence on the uninhibited reaction of any oxide present on the pickled surface will be neglegible. This conclusion is based on the weight-

loss evaluation of unpickled specimens (Fig. 14), which showed that the heavy mill scale was removed in less than 10 minutes following immersion. The completion of scale dissolution was marked by a discontinuity at 0.8 weight percent, as compared to the calculated (Appendix E-2) value of 1.1 weight percent. The calculated value clearly verifies the observation regarding the first discontinuity of Fig. 14. It can therefore be assumed that the freshly pickled specimens did carry an oxide scale which, however, did not have a measurable effect on the weight-loss curves.

The dissolution of the scale is a two-stage reaction. The high temperature mill scale is a multi-layer oxide film[48-a] whose composition may be represented as:

1. FeO next to the metal surface
2. $FeO + Fe_2O_3$ (Fe_3O_4) an intermediate layer and
3. Fe_2O_3 the outermost layer.

The composition change is obviously an oxygen gradient dependent completely on the diffusion of atmospheric oxygen through the film. Mill scale dissolution will thus be:

a) direct dissolution of FeO

$$FeO + 2HCl \longrightarrow Fe^{++} + 2Cl^{-} + H_2O$$

$$\Delta F^{*} = 35{,}360 \text{ cals},$$

* Free energy calculations shown in Appendix E-3

b) electrochemical dissolution (reductive dissolution) in the cell

$Fe/acid/Fe_2O_3$

anode cathode

Cathode reaction: $2H^+ + Fe_2O_3 + 2e^- \longrightarrow 2FeO + H_2O$

$FeO + 2HCl \longrightarrow Fe^{++} + 2CL^- + H_2O$

$\Delta F = -33,710$ cals

Anode reaction: $Fe \longrightarrow Fe^{++} + 2e^-$

$\Delta F = -22,000$ cals

and c) the very slow direct dissolution of Fe_2O_3.

$F = -38,000$ cals

Since the dissolution of the entire mill scale has been shown to be rapid (Fig. 14) and the pickling process satisfactory, the formation of a thin oxide film on the clean coupon surface should follow pickling but should not alter the uninhibited dissolution to any measurable degree.

At each temperature (Figs. 12, 13, 14) two reaction rate zones are apparent:

1. the accelerating rate from 0 weight % loss to 3% loss and
2. the steady rate above 3 weight % loss.

The initial reaction is accelerated because of two features: (a) the presence of deformed metal and (b) an increasing surface area as

dissolution of deformed metal proceeds). Below the region of deformed metal the structure is coarser and therefore offers a more cathodic potential. Thus, as dissolution exposes the more noble sandwich layer, the cathodic to anodic (facial:deformed metal) surface area ratio increases and further accelerates the reaction. At this point a mitigating phenomenon becomes effective, i.e. resistance polarization due to the rapidly reducing anodic area creating a more hindered diffusion. The anodic potential offered by the deformed metal is gradually polarized to the more cathodic potential of the sandwich layer, at which time a joint dissolution of deformed metal and sandwich layer grains takes place. The net effect, shown by the weight-loss curves, is the final transition region from the fast, accelerating initial reaction rate to the slower, constant, second region.

The second zone is marked by a steady rate because of the relatively steady ratio of cathodic to anodic metal surface area. Coupons tested for twenty-four hours in boiling HCl (not shown) still displayed a large amount of the surface skin with the sandwich layer almost absent. The rate is constant over the duration of the tests observed, but at longer immersion times the rate could fall as a higher level of iron in solution is reached. The rate could accelerate as in the case of the first zone, if the ratio of cathodic to anodic surface area is upset. Some evidence of increasing rate was observed in the elevated temperature tests.

During this period, facial surface dissolution begins. As pitting along the edges and on the faces progresses, the coupon takes on a fibrous appearance with the "grain" running along the edges and ends. The overall reaction is not diffusion controlled, since the experimental activation energy was found to be about 13,000 cals./mole.

The iron dissolution is assisted by agitation and increased temperature; the presence of sulfur, evidenced by the numerous grains of Manganese sulfide shown in Figs. 22 to 26, also accelerates corrosion owing to a second, cathode depolarizing reaction

$$2\,H_{ad} + [S^{=}_{S}] \longrightarrow H_2S$$

A mitigating feature of the uninhibited tests is, however, the concentration of ferrous ions building up in the reaction solution. As an illustration, consider the following[47]:

$$Fe \longrightarrow Fe^{++} + 2e^{-} \qquad E^{o}(25^{o}C) = -.6 \text{ volts for } (Fe^{++}) = 1 \text{ mole/litre.}$$

The standard electrode potential of the specimen coupon would be initially lower than -.06 volts on the hydrogen scale. Some time later, however, after perhaps three percent of the coupon has been dissolved, the potential could be ennobled by as much as 0.1 volts. Since the potential is the driving force behind the reaction, the reaction will have a reduced tendency to take place.

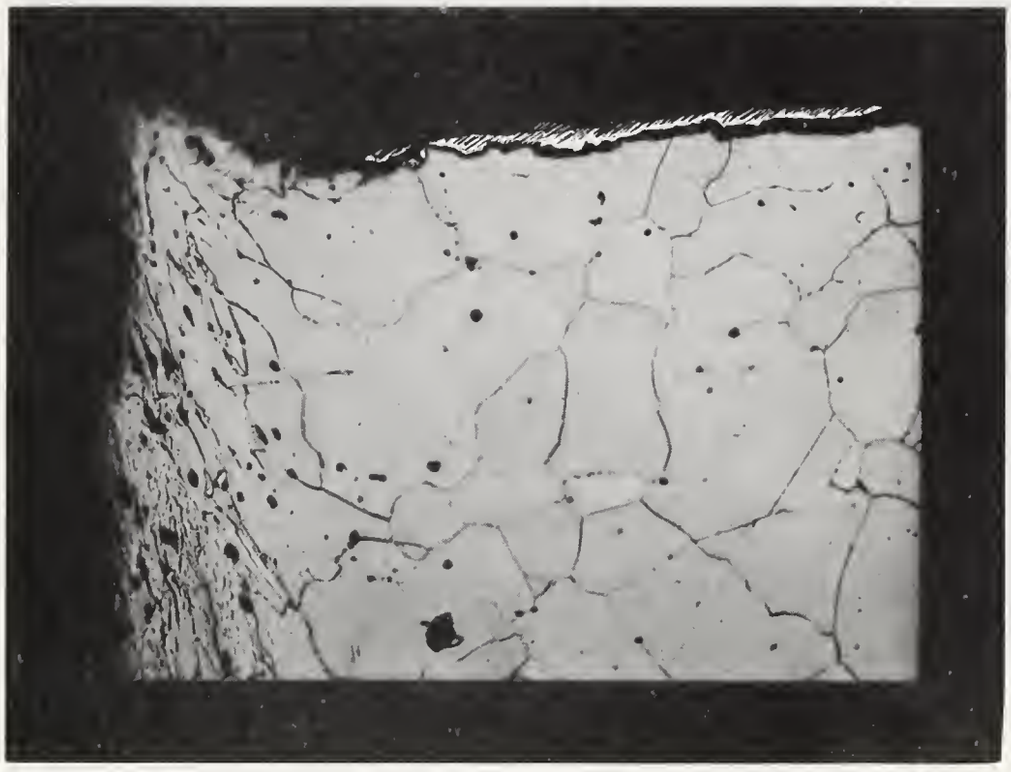

x410

Fig. 22 Edge View of As-Received Lot No. 2 Coupon, Showing Shear Deformation, Oxide Film and Sulfide Inclusions

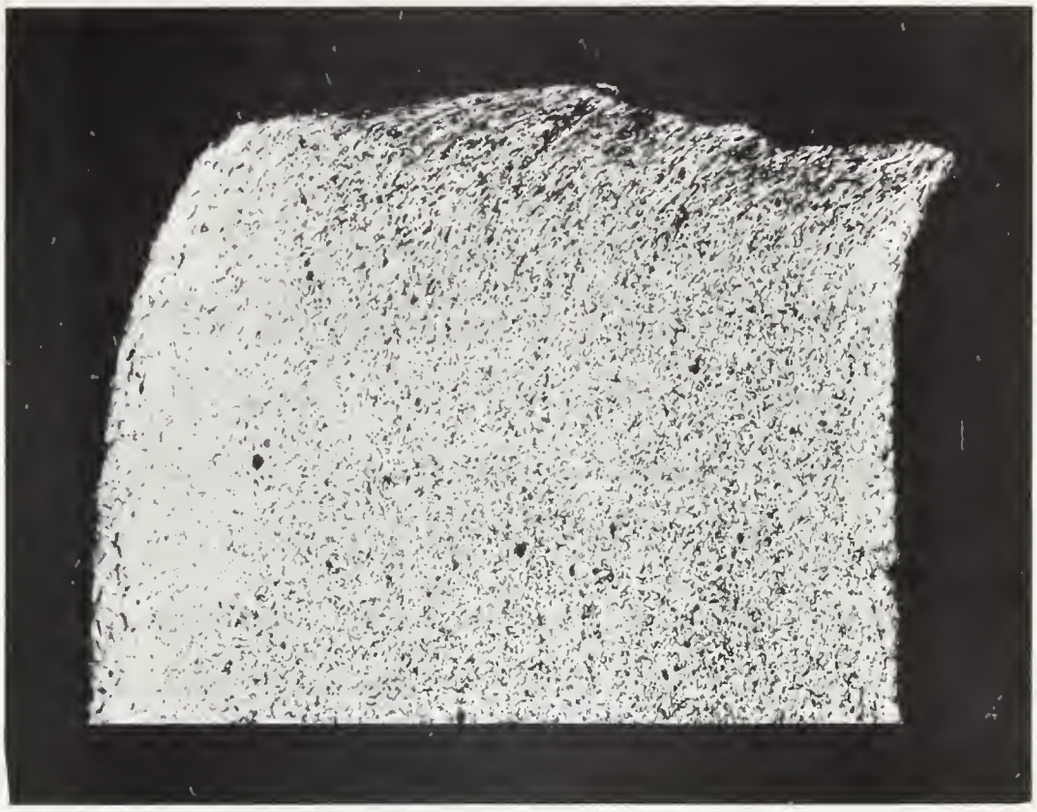

x80

Fig. 23 Edge View of Lot No. 2 As-Received Coupon

x80

Fig. 24 Edge View of Lot No. 2 Coupon After 6 Hours Immersion at 80°C, Uninhibited

THE INHIBITED REACTION

Amine Inhibitors

The significance of the seemingly critical amine chain length (Fig.15) can be discussed in terms of the formation of multiple Van der Waals forces between the hydrocarbon chains. The concentration selected for extensive study (1×10^{-4}M) is, at 60°C, sufficient to develop the optimum protection provided by C_{16} amine. Increasing the chain length to C_{18} offers no additional protection and does, in fact, not quite equal the effect noted with C_{16} amine. This has also been noted by Hackerman, who found an optimum chain length above which corrosion was accelerated. The effect can be explained when one considers the equilibrium that is established between the amine dissociated in solution and the amine present in the micelle structures. Increased hydrocarbon chain length increases the micelle bonding at the same time showing a reduced tendency to go into solution. The net effect is a stronger micelle and reduced adsorption at the solid/liquid interface together with a decreased diffusion rate of the larger molecule. Thus, corrosion may be accelerated if increasingly larger amine molecules are employed, but at a higher temperature, where thermal excitation breaks the micelle bonds, inhibition would be enhanced.

Although the surface sites active for amine adsorption are not affected or in any way changed by the length of the hydrocarbon chain, the film formed by a larger amine molecule would be expected to be more compact and able to bridge larger surface areas (having little or no attraction for amines) than a shorter amine molecule.

Three points of interest are presented:

1. Van der Waals forces between adlineated chains increase with

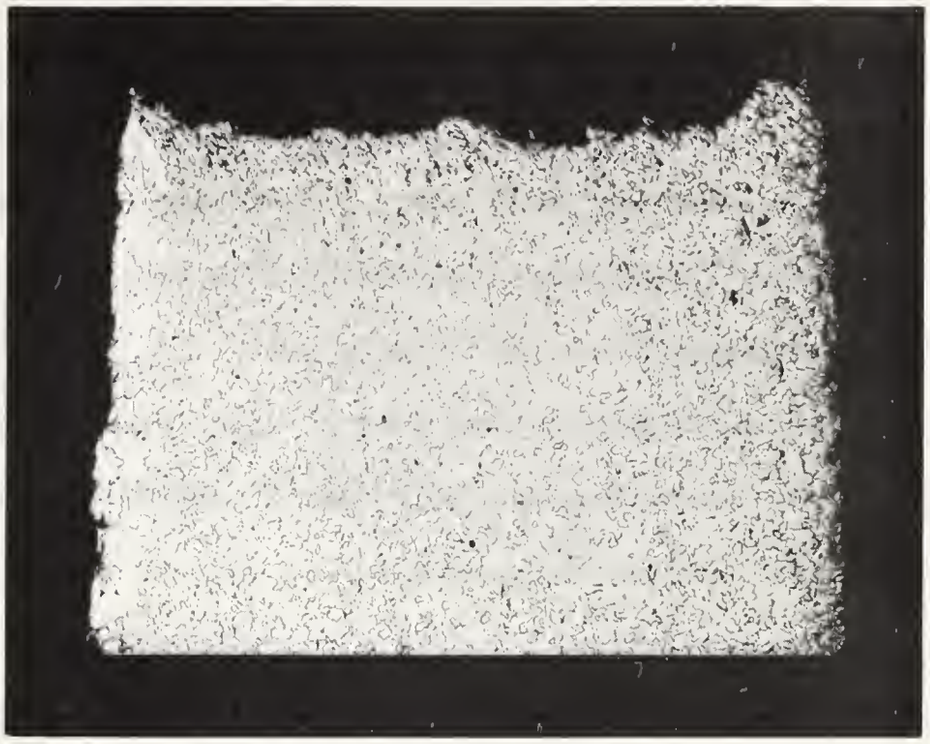

x80

Fig. 25 Edge View of Lot No. 2 Coupon, After 6 Hours Immersion at 60 C, Inhibited C_{I6} Amine

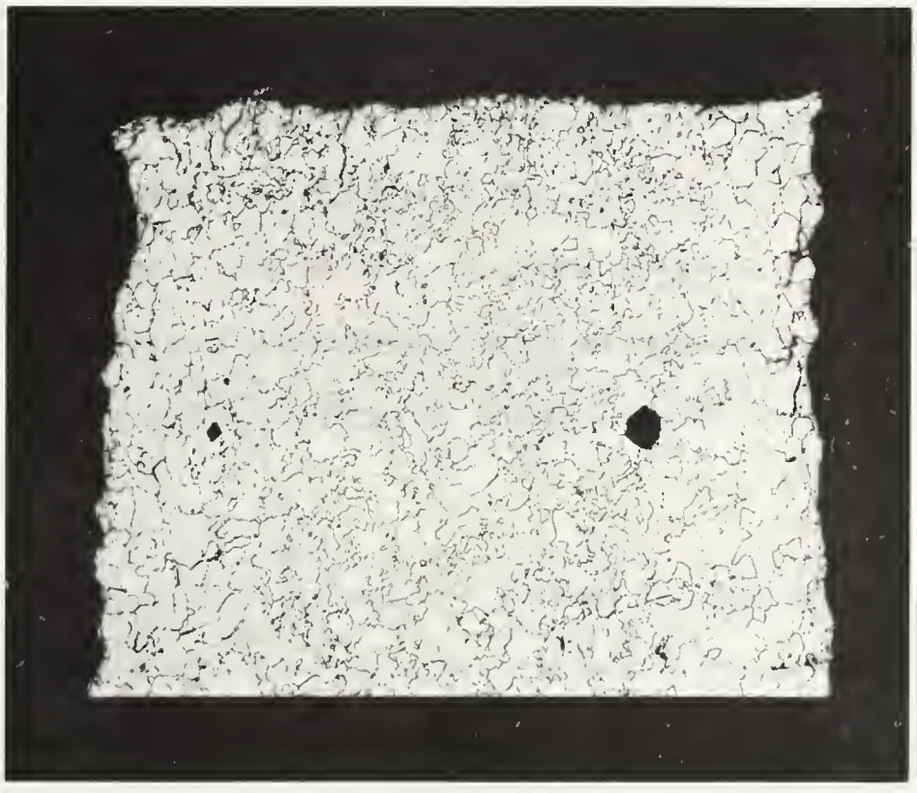

x80

Fig. 26 Edge View of Lot No. 2 Coupon, Annealed I.3 Hours in Argon, at 820 C, After 6 Hours Immersion at 60 C, Inhibited C_{I6} Amine

increasing length of chain. The effect is to solidify, tighten or otherwise restrict the passage for diffusion of reactants and/or products.

2. Amine adsorption does offer a maximum corrosion protection. Increased concentration does not offer increased inhibition but added surfactants do (Fig. 17). The point here is that amine adsorption apparently takes place on a large part of the surface but not on all of it.

3. Di-alkylamines at equivalent concentrations do not offer inhibition comparable to that of the mono-alkylamines. This is due to possible steric hindrance effects resulting from the twin chains and to the reduced number and effectiveness of Van der Waal's cross linking forces.

The adsorbed amine film is not visible but its existence is indicated in the observed surface hydrophobicity. The possibility of a monomolecular film is also suggested by the calculation presented in the previous section and its formation as a result of chemisorptive forces is also supported by the tenacity of the film and its resistance not only to the corrosive environment, but also to the cleaning procedures.

The film offers approximately the same maximum protection at both 60°C and 80° but the temperature does apparently alter the bonding characteristics and the minimum inhibitor concentration is increased at 80°C.

Multicomponent Inhibitors

As was pointed out earlier, the initial results of two and three-component inhibition did not show the anticipated degree of synergistic effect, but the addition of the fourth component did produce such an effect.

The effects are clearly evident in Fig. 17 in which the basic amine component is augmented by C_{18} carboxylic acid, C_{16} alcohol and C_{12} sodium sulfate to produce the best combination at 60°C.

The film formed is stable for a considerable time as evidenced by Fig. 18, but was not protective when the inhibited coupons were removed and placed in an identical uninhibited environment. The reservoir of inhibitor must, clearly, be maintained to service film damage. When this feature is provided, the dissolution process slows drastically - the entire reaction mechanism changing to one of diffusion control with the added possibility of additional support from reaction products being tied up within the film structure.

Evidence of this latter point was apparent in the coloration observed in the multicomponent films. Both the sulfate and phosphate films were multilayers, stable at 60^{o}C in the case of the sulfate and 80^{o} for the phosphate. The bonding forces of the sulfate film were disrupted by increased temperature, while those of the phosphate were apparently reinforced. The increased temperature also affects the minimum concentration of amine required. At 60^{o}C, the minimum amine concentration observed (Fig. 16) was approximately 0.5×10^{-5} molar. In the equimolar four component inhibitor the amine content was 2.5×10^{-5} molar - sufficient for optimum development of the amine-surface bonds to provide coverage and also provide a reservoir of inhibitor. The minimum at 80^{o}C (Fig. 16) was however, 4×10^{-5} molar and thus insufficient amine reagent was present in the equimolar mixture, (Fig. 18-C). The amine content was adjusted to 5×10^{-5} molar and the remaining components reduced to give a total concentration once again of 10×10^{-5} molar. The resulting inhibition (Fig. 19-C) improved markedly.

The existence of micelles in the inhibited solution has been strongly indicated (Fig. 21). These structures are necessary to solubilize otherwise insoluble materials, in this case the acid and alcohol components. Their

presence also alters in an "abnormal" way the electrical, optical and other physical properties of the host solution.

The micelle is a charged agglomerate and appears above the critical micelle concentration (C.M.C.) (a narrow range of composition). The concentration used in the present study exceeded the C.M.C. and thus the equilibrium between the micelle and electrolyte must be considered.

As pointed out by Adamson [37d] there is an equilibrium in effect between surfactant in solution in the diffuse state and the surfactant present in the micelle structures. Increased additions of surfactant beyond the C.M.C. serve only to increase the numbers of micelles present. The micelle, then, in a corrosive environment serves as the required reservoir as mentioned earlier in this discussion.

The foregoing is, of course, only true at temperatures above the Krafft point. This point was found to be between 30 and 40°C in the present case. Below this temperature range, any extra inhibitor addition will precipitate from solution, but at temperatures above 40°C, the extra addition will create additional micelles.

CONCLUSIONS

The results of this study are not absolute proof of the Barrier Film Theory as proposed earlier, but they do provide strong supporting evidence. The main points have been these:

1. With adequate hydrocarbon chain length of the organic inhibitor molecules, sufficient opportunity is provided for the formation of multiple Van der Waals forces between the chains. These forces create an effective diffusion barrier by solidifying the adsorbed film.

2. The use of a combination of molecules having different functional groups has been shown to provide the synergistic effect anticipated, and

3. Corrosion was reduced from 0.45 weight % loss (88.0% inhibition) with C_{16} Amine, to 0.20 weight % loss (94.6% inhibition) with the four component C_{16} Amine, C_{16} Alcohol, C_{18} Acid, C_{12} Sulfate under identical test conditions and at equivalent concentration of inhibitor species.

The suggested mechanism involves the development of lateral strengthening bonds between adjacent functional groups, combined with the lateral Van der Waals forces between hydrocarbon chains to form a solidified barrier film of surfactants. These forces not only create a diffusion barrier but also allow the film to "bridge" surface irregularities and inactive surface sites.

A second effect is provided by the mixed film through the provision of a variety of functional groups which are active at specific surface sites. Since more and varied film surface bonds are provided, the film becomes more firmly attached and its ability to resist adverse environmental conditions becomes more assured.

Thus, the bonding forces, as outlined in the presentation of the Barrier Film Theory, have been supported by this interpretation of the experimental data. It is hoped that in future investigations the multiple re-

flectance techniques of Poling and Leja[34] can be utilized to identify these bonds conclusively.

Since molecular interactions between surfactants have been shown to take place, the effect of multicomponent inhibition will be felt not only in the way that the adsorbed film is anchored to the corroding surface, but also in the micellar structure effects on surface tension. The introduction of sodium dodecyl sulfate, which produces negative dodecyl sulfate ions, causes a reduction of the repulsion forces between the positive polar groups of the amine hydrochloride ions within the micelle structure and at any interface within the system. This, in turn, allows a more complete development of the Van der Waals forces between the hydrocarbon groups and reduces the net charge of the micelle while providing a lowering of the surface tension (Fig. 21). Surface tension is lowered by the replacement of the stronger water dipole-dipole forces at the interface with weaker Van der Waals forces between the extended hydrocarbon chains. Essentially the same effect results from the incorporation of alcohol and carboxylic acid molecules within the micelle structure.

The effect of chain length on surface tension is shown in Fig. 20. By increasing the chain length, the ability of the Van der Waals forces to tighten the micellar structure is increased, while at the interface, increased alignment is created which, in turn, further excludes water from the interfacial film causing a reduction in surface tension. Appendage methyl side chains will have the opposite effect due to steric hindrance.

Similarly, the presence of salts in solution reduces the charge on the functional groups within the micelle and at the interface and thus decreases the repulsion forces. Once again, the Van der Waals forces

create a lowered surface tension.

With reference to corrosion, all of the above features of surface phenomena are effective. The net result of increased chain length, multi-component inhibitors and the presence of salts in the corroding solution is the production of a hydrophobic metal surface, not wetted by solution.

REFERENCES

1. Chappel, E.L., Roetheli, B.E., McCarthy, B.Y., Ind. Eng. Chem, 20, 582 1928

2. Hackerman, N., Corrosion, 8, 143 (1952)

3. Putilova, I.N., Balezin, S.A., Barannik, V.P., Metallic Corrosion Inhibitors, (a) p. 45, (b) p. 46, (c) p. 59, (d) p. 55, Pergamon Press,(1960)

4. Machu, W., Trans. Electrochem. Soc., 72, 333 (1937)

5. Ride, R.N., J. Electrochem. Soc., 103, 98 (1956)

6. Mann, C.A., Trans. Electrochem. Soc., 69, 115 (1936)

7. Chiao Sheh-Jen, Mann, C.A., Ind. Eng. Chem., 39, 910 (1947)

8. Mann, C.A., Lauer, B.E., Hultin, C.T., Ind. Eng. Chem, 28, 159 (1936)

9. Mann, C.A., Lauer, B.E., Hultin, C.T., Ind. Eng. Chem, 28, 1048 (1936)

10. Hackerman, N., Sudbury, J.D., J. Electrochem. Soc., 97, 109 (1950)

11. Kaeshe, H., Hackerman, N., J. Electrochem. Soc., 105, 191 (1958)

12. Cavallaro, L., Bolognesi, G., Atti. accad. sci. Ferrara, 24, No. 1, (1946-47)

13. Hoar, T.P., Pittsburgh International Conference on Surface Reactions, p. 127, Pittsburgh Corrosion Publishing Co., (1948)

14. Kuznetsov, V.A ., Lofa, Z.A., J. Phys. Chem. (U.S.S.R.), 21, 201 (1947)

15. Bordeaux, J.J., Hackerman, N., J. Phys. Chem., 61, 1323 (1957)

16. Hackerman, N., Cook, E.L., J. Electrochem. Soc., 97, 1 (1950)

17. Hackerman, N., Cook, E.L., J. Phys. Chem., 56, 524 (1952)

18. Greenhill, E.B., Trans. Faraday Soc., 45, 625 (1949)

19. Dintenfass, L., Chemistry and Industry, May 4, 560, (1957)

20. Hackerman, N., Makrides, A.C., Ind. Eng. Chem., 46, 523 (1954)

21. Jimeno, E., Grifoll, I., Moralle. F.R., Trans. Electrochem. Soc., 69 105, (1936)

22. Hackerman, N., Sudbury, J.D., J. Electrochem. Soc., 93, 191 (1948)

23. Swearigen, L.E., Schram. A.F., J. Phys. Colloid Chem., 54, 180 (1950)

24. Hackerman, N., Hurd, R.M., Annond, R.R., Corrosion, 18, 37t (1962)

25. Hackerman, N., Corrosion, 18, 332t (1962)

26. Rhodes, F.H., Kuan, W.E., Ind. Eng. Chem., 21, 1066 (1929)

27. Cardwell, P.H., Eilers, L.A., Ind. Eng. Chem., 40, 1951 (1948)

28. Riggs, O.L., Every, R.L., Corrosion, 18, 262t (1962)

29. Foster, G.L., Oakes, B.D., Kucera, C.H., Ind. Eng. Chem., 51, 825 (1959)

30. Hackerman, N., Schmid, H.R., Corrosion, 5, 237 (1949)

31. Maxted, E.B., J. Chem. Soc., 1987 (1949)

32. Faraday, Phil. Mag., 9, 61 (1936)

33. Leja, J., Schulman, J.A., Trans. A.I.M.E., Feb., 221 (1954)

34. Poling, G.W., Leja, J., Can. Met. Quarterly, 1, 109 (1962)

35. Shwoegler, E.J., Berman, L.U., Corrosion, 15, 128t (1959)

36. Ayers, R.C., Hackerman, N., J. Electrochem. Soc., 110, 507 (1963)

37. Adamson, A.W., Physical Chemistry of Surfaces, Interscience Publishers (1963): (a) p. 344, (b) p. 142, (c) p. 344, (d) p. 373.

38. Zisman, W.A., J. Chem. Phys., 9, 534 (1941)

39. Zisman, W.A., J. Chem. Phys., 9, 729 (1941)

40. Zisman, W.A., J. Chem. Phys., 9, 789 (1941)

41. Bigelow, W.C., Pickett, D.L., Zisman, W.A., J. Colloid Sci., 1, 513 1946

42. Bigelow, W.C., Glass, E., Zisman, W.A., J. Colloid Sci, 2, 563 (1947)

43. Shafrin, E.G., Zisman, W.A., Monomolecular Layers, p. 129: A symposium presented Dec. 27, 1951 at the Philadelphia meeting of American Association for Advancement of Science, (1954)

44. Ardagh, E.G.R., Roome, R.M.B., Owens, H.W., Ind. Eng. Chem., 25, 1116 (1933)

45. Handbook of Physics and Chemistry, 44, 3422, (1962)

46. Epstein, H.T., J. Phys. Chem., 54, 1053 (1950)

47. Pourbaix, M.J.N., Thermodynamics of Dilute Aqueous Solutions, Edward Arnold and Co., (1949)

48. Kubaschewski, O., Hopkins, B.E., Butterworths (1962) (a) p. 3, (b) p. 38, (c) p. 10

49. Harkins, W.D., Brown, F.E., J. American Chem. Soc., 41, 499 (1919)

50. Evans, U.R.,The Corrosion and Oxidation of Metals, (a) p. 87, (b) p. 225

51. Harkins, W.D., The Physical Chemistry of Surface Films, Reinhold (1954)

APPENDIX A

TABLE A-1

TYPICAL ANALYSIS OF COUPON SPECIMENS

SAMPLE	Analysis Percent		
	A	B	C
Carbon	0.04	0.04	0.04
Manganese	0.31	0.30	0.31
Phosphorous	0.016	0.014	0.018
Sulfur	0.050	0.056	0.054
Silicon	0.05	0.05	0.05

APPENDIX B

STUDY OF THE VARIABLES AFFECTING THE UNINHIBITED CORROSION RATE

TABLE B-1

PRELIMINARY EVALUATION - LOT NO. 1 SPECIMENS

Mixer Speed - 900 to 1100 rpm

Temperature - 60 ± 5°C

Immersion Time - 13 Hours

INITIAL SAMPLE WEIGHT (Grams)	WEIGHT-LOSS (Percent)
5.55	10.19
5.56	10.35
5.54	11.87
5.58	11.88
5.57	9.80
5.58	9.67
5.64	11.70
5.58	12.18
5.54	15.72
5.57	14.69
5.53	13.45
5.60	13.51
5.52	8.06
5.46	7.84

Average - 11.49%

Range - ± 3.94%

These tests were conducted in duplicate and the results clearly display pairing. The range of the results is not only too large, but the frequency distribution is far from an idealized normal curve.

TABLE B-2

EFFECT OF MIXER SPEED

Mixer Speed - High, low

Temperature - 60°C

Immersion Time - 6 Hours

	1175 rpm		550 rpm	
	Initial Sample Weight (gms)	Weight-Loss %	Initial Sample Weight (gms)	Weight-Loss %
	5.41	3.96	5.42	3.47
	5.35	3.84	5.39	3.02
	5.40	4.00	5.47	4.27
	5.46	4.15	5.40	4.16
	5.41	3.71	5.44	3.88
	5.35	3.88	5.36	4.02
	5.44	4.35	5.43	3.74
	5.44	4.48	5.31	3.81
	5.44	3.65	5.29	3.97
	5.33	3.82	5.46	3.61
	5.41	3.62	5.42	3.52
	5.34	3.85	5.45	3.72
Av.	5.40	3.94	5.40	3.77

STUDENTS' t TEST FOR COMPARISON

OF THE MIXER SPEED DATA

	1175 rpm	550 rpm
Average Sample Weight	5.40	5.40
Average Weight-Loss %	$\bar{x} = 3.94$	$\bar{y} = 3.77$
	$\sum x^2 = 187.46$	$\sum y^2 = 177.44$
	$\left(\frac{\sum x^2}{n_x}\right) = 186.68$	$\left(\frac{\sum y^2}{n_y}\right) = 170.18$

$$\sigma^2 = \frac{(171.44 - 170.18) - (187.46 - 186.68)}{(n_x + n_y - 2)}$$

$$= \frac{0.4826}{22}$$

$$\sigma^2 = 0.0219$$

$$\sigma = 0.148$$

$$t = \frac{3.944 - 3.77}{0.148} \sqrt{\frac{12(12)}{24}}$$

$$= \frac{0.178}{0.1481} \sqrt{6} = 2.94$$

$t = 2.94$ for 22 degrees of freedom

Therefore: the difference between the means is significant to between the 99.0 and 99.9% confidence limits.

VARIANCE ANALYSIS

To determine whether the variation in the results with fast mixing differs from that of slow mixing, a variance analysis was carried out. Assume that the variabilities of data from each test procedure are the same, then:

$$\sigma_x^2 = \frac{187.46 - 186.68}{n_x - 1} = \frac{0.78}{11} = 0.0709$$

$$\sigma_y^2 = \frac{171.44 - 170.18}{n_y - 1} = \frac{1.262}{11} = 0.106$$

$$\text{The variance ratio } F = \frac{0.016}{0.0709} = 1.49$$

The hypothesis that the two sets of data are comparable has not been disproved since the variance ratio F falls below the 98% significance level.

TABLE B-3

UNINHIBITED CORROSION - LOT NO. 2 SPECIMENS

Mixer Speed - 1,000 rpm
Temperature - 60°C
Immersion Time - 6 Hours

INITIAL SAMPLE WEIGHT (grams)	WEIGHT-LOSS (percent)
5.28	3.75
5.37	3.75
5.40	3.91
5.28	3.74
5.43	3.65
5.49	3.68
5.39	3.60
5.33	3.70
5.42	3.81
5.39	3.73
5.41	3.91
5.30	3.60
5.44	3.77
5.40	3.55
5.46	3.36
5.41	3.96
5.35	3.86
5.40	4.00
5.46	4.15
5.41	3.71
5.35	3.88
5.44	3.65
5.33	3.82
5.41	3.62
5.34	3.85
5.42	3.47
5.40	4.16
5.44	3.88
5.36	4.02
5.43	3.74
5.31	3.87
5.29	3.97
5.46	3.61
5.42	3.52
5.45	3.72
Average	3.77
Range	0.80

TABLE B-4

FREQUENCY ANALYSIS OF UNINHIBITED CORROSION RATE

LOT NO. 2 SPECIMENS

Temperature - 60°C

Immersion Time - 6 Hours

WEIGHT-LOSS RANGE	FREQUENCY
3.11 - 3.20	0
3.21 - 3.30	0
3.31 - 3.40	1
3.41 - 3.50	1
3.51 - 3.60	4
3.61 - 3.70	6
3.71 - 3.80	8
3.81 - 3.90	7
3.91 - 4.00	5
4.01 - 4.10	1
4.11 - 4.20	2
4.21 - 4.30	1

The significant feature of these results lies in the fact that they fortunately do follow a normal distribution pattern and that, although the range of the results (0.80%) is fairly wide, the average value (3.77) corresponds with that of the mode (3.71 - 3.80) and the median value (3.8).

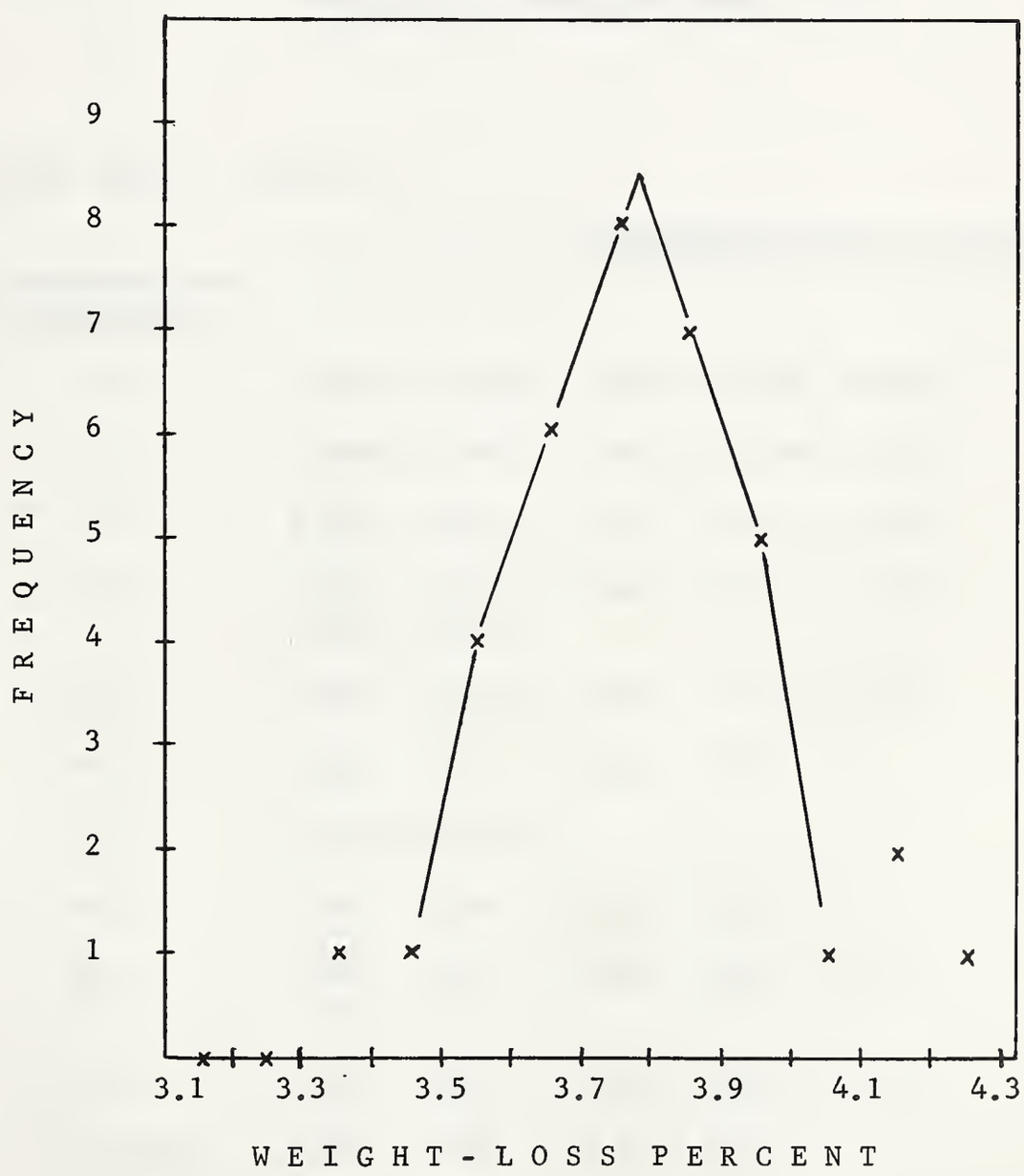

Fig. 27 Frequency Distribution, Uninhibited Corrosion, Lot No. 2 Specimens, After 6 Hours Immersion at 60°C.

APPENDIX C

EVALUATION OF THE EFFECT OF TEMPERATURE ON THE UNINHIBITED CORROSION RATE

TABLE C-1

UNINHIBITED CORROSION RATE - 60°C

Mixer Speed - 1,000 rpm

Immersion Time (minutes)	WEIGHT-LOSS DATA (percent)	Average	Median
15	0.0496, 0.0524, 0.0539, 0.0549, 0.0610	0.0544	0.0539
30	0.0947, 0.0975, 0.0976, 0.1019, 0.1070	0.0997	0.0976
60	0.219, 0.225, 0.229, 0.253, 0.263	0.237	0.229
120	0.474, 0.478, 0.545, 0.545, 0.556, 0.559, 0.584	0.534	0.545
240	0,984, 0.989, 1.073, 1.175, 1.192	1.083	1.073
300	1.82, 1.97, 2.22, 2.46	2.12	
360	(See Table B-3)	3.77	
480	4.90, 4.94, 4.95, 5.11, 5.11	5.00	4.95
600	4.98, 5.11, 5.20, 5.61, 5.79, 6.01	5.45	5.20
720	5.85, 6.07, 6.11, 6.21, 6.33	6.11	6.11
22 hours	9.37, 9.83, 10.7, 10.8	10.2	

TABLE C-2

UNINHIBITED CORROSION RATE - 80°C

Mixer Speed - 1,000 rpm

Immersion Time (minutes)	WEIGHT-LOSS DATA (percent)	Average	Median
10	0.168, 0.177	0.172	
15	0.222, 0.230	0.226	
17	0.252, 0.273	0.262	
20	0.243, 0.252, 0.265, 0.280, 0.280	0.264	0.265
23	0.362, 0.409	0.386	
40	0.568, 0.590	0.579	
46	0.585, 0.600	0.592	
51	0.775, 0.693	0.734	
80	1.01, 1.02, 1.08, 1.12, 1.13	1.07	1.08
100	1.33, 1.34	1.33	
106	1.31, 1.28	1.30	
110	1.43, 1.47	1.45	
140	2.91, 3.15, 3.22, 3.22, 3.44	3.19	3.22
200	3.63, 3.93, 4.06, 4.09, 4.23	3.99	4.06
260	5.21, 5.33, 5.43, 5.45	5.37	5.33
320	6.06, 6.14, 6.25, 6.29	6.15	6.14
530	9.38, 9.78, 9.89, 9.89	9.74	9.78
590	9.18, 9.61, 10.29, 10.99, 10.87, 11.11	10.34	
560	10.61, 11.31, 12.11, 12.11, 12.45	11.72	

TABLE C-3

UNINHIBITED CORROSION RATE - 90°C

Mixer Speed - 1,000 rpm

Immersion Time (minutes)	WEIGHT-LOSS DATA (percent)	Average
5	0.0554, 0.0943	0.0748
15	0.215, 0.348	0.282
25	0.463, 0.700	0.581
35	0.765, 1.122	0.942
50	1.22, 1.72	1.47
65	1.78, 2.45	2.12
80	2.38, 3.22	2.80
95	2.68, 3.52	3.10
115	3.10, 3.96	3.53
135	3.52, 4.42	3.97
195	4.91, 5.91	5.41
330	9.9, 11.2	10.5

TABLE C-4

UNINHIBITED CORROSION RATE - 95°C

Mixer Speed - 1,000 rpm

Immersion Time (minutes)	WEIGHT-LOSS DATA(percent)	Average
5	0.166, 0.183, 0.187	0.179
10	0.339, 0.366, 0.368, 0.437	0.378
15	0.398, 0.408, 0.516, 0.529, 0.518, 0.646	0.502
20	0.619, 0.675, 0.679, 0.686	0.663
25	0.650, 0.661, 1.21, 1.24	0.94
30	0.835, 0.893, 0.911, 1.02, 1.41, 1.43, 1.49	1.19
35	1.57, 1.60, 1.64, 1.88	1.67
40	1.83, 1.87, (1.06, 1.11, 1.36, 1.40)*	1.85
45	2.03, 2.08	2.05
50	2.23, 2.26, 2.27	2.25
60	(1.58, 1.53, 2.02, 2.11)	
65	2.44, 2.76	2.60
80	2.82, 3.12, (1.98, 1.95, 2.02, 2.00)	2.97
90	3.22, 3.35, (2.15, 2.18)	3.28
100	(2.36, 2.35)	
110	3.66, 4.21	3.93
120	4.82, 5.44, (2.60, 2.72)	5.13
140	(3.02, 3.06)	
150	(8.32, 6.54)	
185	6,54, 6.61	6.57
200	6.77, 7.10	6.93
255	8.73, 8.94	8.83
270	(14.2, 14.4)	

* not included in average

APPENDIX D

CORROSION OF UNPICKLED SPECIMENS

TABLE D-1

UNINHIBITED CORROSION RATE - 90°C

Mixer Speed - 1,000 rpm

Immersion Time (minutes)	WEIGHT-LOSS DATA (percent)	Average
5	0.800, 0.835	0.817
10	1.02, 1.03	1.02
20	1.48, 1.51	1.49
30	1.87, 1.93	1.90
40	2.32, 2.39	2.35
50	3.27, 3.40	3.33
65	4.07, 4.21	4.14
102	6.33, 6.51	6.42

APPENDIX E-1

ESTIMATION OF SHEAR DEFORMED METAL

In order to justify the explanation of the discontinuity in the various uninhibited weight-loss studies, the following estimate of shear deformed metal volume was carried out based on estimates of the extent of deformation as observed under high magnification of sample sections.

Estimated extent of deformation: 0.015 cm

Average specimen dimensions:

length	3.82 cm
width	1.32 cm
thickness	0.153 cm

$$\text{Deformed metal volume} = \left[1.32(0.153)\ 0.015\right] 2 + \left[3.79(0.153)0.015\right] 2$$

$$= 0.0235\ \text{cm}^3$$

$$\text{Total coupon volume} = 1.32(0.153)3.82 = 0.773\ \text{cm}^3$$

$$\text{Deformed metal volume} = \frac{0.0235(100)}{0.773} = 3.0\% \text{ of the total coupon volume.}$$

Assuming that the densities of both shear deformed metal and normal metal are identical, the shear deformed metal will therefore represent approximately 3% by weight of the total coupon weight.

APPENDIX E-2

ESTIMATION OF OXIDE MILL SCALE

Assume that the scale is completely FeO

FeO specific volume = 12 cc/mole (48 C)

Scale dimensions = $3.82 \times 1.32 \times 1 \times 10^{-3}$ cm

(thickness, 1×10^{-3} cm, estimated from Fig. 22, other dimension from caliper measurements of specimens)

Total scale volume = 10.1×10^{-3} cm^3

$$\text{Mill scale} = \frac{10.1 \times 10^{-3}}{12}$$

$$= 0.84 \times 10^{-3} \text{ moles FeO}$$

$$\text{Weight of oxide} = 0.84 \times 10^{-3} (55.9 + 16)$$

$$= 60.4 \times 10^{-3} \text{ gms}$$

Average pickled specimen weight = 5.5 gms

Calculated weight-loss due to scale dissolution only

$$= \frac{0.0604}{5.56} (100) = 1.1 \text{ weight \%}$$

APPENDIX E-3

STANDARD CHEMICAL POTENTIALS (47)

	25^{o}C (cals./mole)
H_2O	- 56,560
HCl	- 22,740
$Cl^{-}aq$	- 31,345
$H^{+}aq$	0
(H_2)	0
Fe	0
$Fe^{++}aq$	- 20,310
Fe O	- 58,720
Fe_2O_3	-176,100

APPENDIX E-4

MILL SCALE DISSOLUTION

(a) $FeO + 2\ HCl \longrightarrow Fe^{++} + 2\ Cl^{-} + H_2O$

$$\Delta F^{\circ} = \left[-20{,}310 - 2(31{,}345) - 56{,}560\right] + \left[58{,}720 + 2(22{,}740)\right]$$

$$\Delta F^{\circ} = -35{,}360 \text{ cals.}$$

At equilibrium $\Delta F^{\circ} = -RT \ln K$

$$\therefore \log K = -\frac{(-35{,}360)}{2.303(1.98)298} = +\frac{(35{,}360)}{1{,}363} = 25.09$$

At $60^{\circ}C$ $\Delta F = \Delta F^{\circ} + RT \ln K$

$$= -35{,}360 + \frac{1.98(333)}{2.303} \log \frac{\left[Fe^{++}\right]\left[Cl^{-}\right]^2}{\left[FeO\right]\left[HCl\right]^2}$$

Assume activity = molar concentration

Total Volume = 1 litre of pickling solution

Acid added = $\frac{1}{2}$ litre $= \frac{500(1.188)\ 0.37}{36.5} = 6.01$ moles HCl

$$\therefore HCl = 6.01$$

Assume HCl completely dissociated

$$\left[Cl^{-}\right] = 6.01$$

thus $$\Delta F_{60^{\circ}C} = -35{,}360 + 287 \log \left[Fe^{++}\right]$$

and $$\left[Fe^{++}\right] \approx 0$$

thus

$$\Delta F_{60^{\circ}C} \approx -35{,}360 \text{ cals.}$$

(b) Cathodic reaction

$$Fe_2O_3 + 2\ H^+ + 2\ e^- \longrightarrow 2FeO + H_2O$$

$$\Delta F^o = (176,100 + 2\ (0) - (2\ (58,720) + 56,560)$$

$$= 176,100 - 174,000 = + 2,100 \text{ cals}$$

$$\Delta F_{60^oC} = \Delta F^o + RT \ln K$$

$$= 2,100 + 287 \log \frac{1}{\left[H^+\right]^2}$$

Assume as in (a) that activity = concentration and that the HCl dissociates completely

$$\left[H^+\right] = 6.01$$

thus $\Delta F_{60^oC} = 2,100 + 287 \log \frac{1}{(6.01)^2} = 2,100 - 447 = + 1,650$ cals

Anodic reaction

$$Fe \longrightarrow Fe^{++} + 2e^-$$

$$\Delta F^o = -20,310$$

$$\Delta F_{60^oC} = -20,310 + RT \ln \frac{\left[Fe^{++}\right]}{1}$$

Assume $\left[Fe^{++}\right] = 1 \times 10^{-6}$ M

$$F_{60^oC} = -20,310 + 287 \log 1 \times 10^{-6} = -20,310 - 1,720 = -22,000 \text{ cals}$$

(c) $Fe_2O_3 + 6H^+ + 4\ Cl^- \longrightarrow 2Fe^{++} + 4\ Cl^- + 3\ H_2O$

$$\Delta F^\circ = 176{,}100 + 6(0) - 2(20{,}310) - 3(56{,}560)$$

$$\Delta F^\circ = -34{,}200$$

$$\Delta F_{60^\circ C} = -34{,}200 + RT \ln \frac{[Fe^{++}]^2}{[H^+]^6}$$

$$\Delta F_{60^\circ C} = -34{,}200 + 287 \log \frac{[10^{-6}]^2}{[6]^6} = -38{,}000 \text{ cals}$$

APPENDIX F

STUDY OF THE EFFECTS OF TIME, TEMPERATURE

AND INHIBITOR CONCENTRATION ON INHIBITED CORROSION RATES

TABLE F-1

COMPARISON BETWEEN MONO AND DI-ALKYL AMINES

AND THE EFFECT OF CHAIN LENGTH

Total Concentration of Inhibitor - 10^{-4} molar
Mixer Speed - 1,000 rpm
Temperature - 60°C
Immersion Time - 6 hours

	Reagent	Molecular Weight	WEIGHT-LOSS DATA (Percent) 1	2	3	4	5	6	7	Average W-Loss %	Median W-Loss %	Average Inhib. %
1.	C_6	101.19	3.28	3.31	3.32	3.39	3.57	3.57		3.41	3.32	9.54
2.	di C_3	101.19	3.86	3.90	3.90	3.98	3.99	4.01		3.94	3.90	-4.51
3.	C_{10}	157.29	2.89	2.91	2.98	3.04	3.05	3.06	3.08	3.00	3.04	20.2
4.	di C_6	185.35	2.82	2.85	2.96	3.08	3.09	3.09		2.98	2.96	21.0
5.	C_{16}	241.45	0.415	0.426	0.457	0.468	0.479	0.480		0.454	0.457	88.0
6.	C_{18}	269.50	0.479	0.501	0.501	0.504	0.513			0.500	0.501	86.7

TABLE F-2

CRITICAL INHIBITOR CONCENTRATION

Mixer Speed - 1,000 rpm
Temperature - 60 and 80° C
Immersion Time - 6 Hours

Reagent C_{16} Amine Concentration	WEIGHT-LOSS DATA (Percent) 1	2	3	4	5	6	7	8	Average W-Loss %	Median W-Loss %	Average Inhib. %
60 degrees Centigrade											
1. (0.121 gms/l.) 0.5×10^{-3} M	0.427	0.464	0.469	0.482	0.488	0.497	0.513	0.540	0.485	0.482	86.9
2. (0.0241gms/l.) 10^{-4} M	0.415	0.426	0.457	0.468	0.479	0.480			0.454	0.457	88.0
3. (0.012 gms/l.) 0.5×10^{-4} M	0.400	0.425	0.477	0.485	0.487	0.490			0.461	0.477	87.8
4. (0.003 gms/l.) 0.25×10^{-4} M	0.397	0.401	0.412	0.426	0.436	0.446	0.461		0.426	0.426	88.5
5. (0.0012gms/l.) 0.5×10^{-5} M	0.97	0.99	1.05	1.11	1.11	1.13	1.15	1.18	1.09	1.11	71.1
80 degrees Centigrade											
1. (0.060 gms/l.) 0.25×10^{-3} M	0.411	0.422	0.434	0.436	0.436	0.442			0.430	0.434	93.5
2. (0.024 gms/l.) 1×10^{-4} M	0.425	0.450	0.456	0.469	0.470	0.484	0.508	0.516	0.472	0.469	92.9
3. (0.012 gms/l.) 0.5×10^{-4} M	0.454	0.485	0.508	0.527					0.494		92.5
4. (0.0024gms/l.) 1×10^{-5} M	4.34	5.15	5.73	6.49					5.43		17.7

TABLE F-3

COMBINED AMINE AND CARBOXYLIC ACID INHIBITION

Total Concentration of Inhibitors (equimolar) - 10^{-4} M

Mixer Speed - 1,000 rpm

Temperature - 60°C

Immersion Time- 6 Hours

	Reagent		WEIGHT-LOSS DATA (Percent)									
	Amine	Acid	1	2	3	4	5	6	7	Average W-Loss %	Median W-Loss %	Average Inhib. %
1.	C_{16}	C_{10}	0.465	0.481	0.486	0.495	0.515	0.518	0.528	0.498	0.495	86.6
2.	C_{16}	C_{12}	0.462	0.468	0.486	0.487	0.487	0.496	0.511	0.485	0.487	86.9
3.	C_{16}	C_{14}	0.455	0.485	0.494	0.495	0.497	0.509		0.489	0.494	86.9
4.	C_{16}	C_{18}	0.473	0.478	0.481	0.481	0.492	0.493	0.500	0.485	0.481	86.9

TABLE F-4

COMBINED AMINE, CARBOXYLIC ACID AND ALCOHOL INHIBITION

Total Concentration of Inhibitors (equimolar) - 10^{-4} M

Mixer Speed - 1,000 rpm

Temperature - 60°C

Immersion Time- 6 Hours

	Reagent			WEIGHT-LOSS DATA (Percent)									
	Amine	Acid	Alcohol	1	2	3	4	5	6	7	Average W-Loss %	Median W-Loss %	Average Inhib. %
1.	C_{16}	C_{14}	C_{12}	0.413	0.425	0.436	0.441	0.474			0.438	0.436	88.3
2.	C_{16}	C_{18}	C_{16}	0.438	0.448	0.471	0.475	0.480	0.486	0.509	0.472	0.47	87.5
3	C_{16}	C_{14}	C_{16}	0.478	0.497	0.500	0.520	0.531	0.536	0.552	0.516	0.520	86.1

TABLE F-5

COMBINED AMINE, CARBOXYLIC ACID,

ALCOHOL AND SULFATE INHIBITION

Total Concentration of Inhibitors (equimolar) - 10^{-4} M

Mixer Speed - 1,000 rpm

Temperature - 60°C

Immersion Time- 6 Hours

	Reagent				WEIGHT-LOSS DATA (Percent)								
	Amine	Acid	Alcohol	$RNaSO_4$	1	2	3	4	5	6	Average W-Loss %	Median W-Loss %	Average Inhib. %
1.	C_{16}	C_{14}	C_{12}	C_{12}	0.397	0.419	0.440	0.445	0.446	0.478	0.437	0.440	88.3
2.	C_{16}	C_{14}	C_{16}	C_{12}	0.279	0.282	0.290	0.292	0.304	0.311	0.293	0.290	92.4
3.	C_{16}	C_{18}	C_{16}	C_{12}	0.166	0.183	0.195	0.223	0.243		0.202	0.195	94.6

TABLE F-6

COMBINED AMINE SULFATE AND AMINE PHOSPHATE INHIBITION

Total Concentration of Inhibitor (equimolar) - 10^{-4} M

Mixer Speed - 1,000 rpm

Temperature - 60°C

Immersion Time- 6 Hours

Reagent	WEIGHT-LOSS DATA (Percent)								Average W-Loss %	Median W-Loss %	Average Inhib. %
	1	2	3	4	5	6	7	8			
1. C_{16} Amine Mono and di C_{13} Phosphate	0.404	0.414	0.415	0.420	0.435	0.435	0.464	0.471	0.430	0.420	88.8
2. C_{16} Amine C_{12} Sulfate	0.514	0.523	0.537	0.541	0.545	0.565	0.566	0.606	0.539	0.541	85.6

TABLE F-7

EFFECT OF IMMERSION TIME AND TEMPERATURE

ON MULTICOMPONENT INHIBITION

Total Concentration of Inhibitors (equimolar) 10^{-4} M
Mixer Speed - 1,000 rpm
Temperature 60 and 80°C

Reagent	WEIGHT-LOSS DATA (Percent) 1	2	3	4	5	6	Average W-Loss %	Average Inhib. %
6 hours 60°C								
1. C_{16} Amine, C_{16} Alcohol C_{18} Acid, C_{12} Sulfate	(See Table F-5)						0.202	94.6
2. C_{16} Amine, C_{16} Alcohol C_{18} Acid, C_{13} Phosphate*	0.273	0.279	0.299	0.305			0.289	92.4
10 hours 60°C								
3. C_{16} Amine, C_{16} Alcohol C_{18} Acid, C_{12} Sulfate	0.166	0.245	0.248	0.315			0.244	95.6
4. C_{16} Amine, C_{16} Alcohol C_{18} Acid, C_{13} Phosphate	0.581	0.591	0.606	0.610	0.643	0.651	0.613	88.9

..continued..

Table F-7 ..conclusion..

Reagent	WEIGHT-LOSS DATA (Percent) 1	2	3	4	5	6	Average W-Loss %	Average Inhib. %
12 hours 60°C								
5. C_{16} Amine, C_{16} Alcohol, C_{18} Acid, C_{12} Sulfate	0.290	0.328					0.309	94.9
16 hours 60°C								
6. C_{16} Amine, C_{16} Alcohol, C_{18} Acid, C_{12} Sulfate	0.313	0.281					0.297	96.2
7. C_{16} Amine, C_{16} Alcohol, C_{18} Acid, C_{13} Phosphate	1.01	1.03	1.09	1.07			1.05	85.9
6 hours 80°C								
8. C_{16} Amine, C_{16} Alcohol, C_{18} Acid, C_{12} Sulfate	1.71	1.53	1.47	1.54	(2.16	4.16)+	1.56	76.4
9. C_{16} Amine, C_{16} Alcohol, C_{18} Acid, C_{13} Phosphate	1.28	1.33	1.20	0.96	1.51	1.63	1.32	80.8

* mixed mono and di C_{13} phosphate

\+ bracketed figure not incorporated in average

TABLE F-8

EFFECT OF IMMERSION TIME, TEMPERATURE AND CONCENTRATION

ON MULTICOMPONENT INHIBITION

Reagent	WEIGHT-LOSS DATA (Percent) 1	2	3	4	5	6	Average W-Loss %	Average Inhib. %
6 hours 60°C								
1. (equimolar) C_{16}Amine, C_{16}Alcohol C_{18} Acid, C_{12}Sulfate	See Table F-5						0.202	94.6
2. (equimolar) C_{16}Amine, C_{16}Alcohol C_{18}Acid, C_{13}Phosphate*	See Table F-7						0.289	92.4
3. $0.5x10^{-4}$M C_{16} Amine $0.5x10^{-4}$M C_{16}Alcohol, C_{18} Acid C_{12} Phosphate	0.384	0.389	0.429	0.433			0.409	89.1
10 hours 60°C								
4. $0.5x10^{-4}$M C_{16} Amine $0.5x10^{-4}$M C_{16} Alcohol C_{18} Acid, C_{13} Phosphate	0.638	0.638	0.676	0.691	(0.725	0.725)+	0.661	87.8

* mono and di-alkyl phosphate

+ bracket figures not incorporated in average

..continued..

Table F-8 ..conclusion..

Reagent	WEIGHT-LOSS DATA (Percent) 1	2	3	4	5	6	Average W-Loss %	Average Inhib. %
6 hours 80°C								
1. 0.5×10^{-4} M C_{16} Amine 0.5×10^{-4} M C_{16} Alcohol, C_{18} Acid C_{12} Sulfate	0.93	0.97	1.02	(1.28)+			0.97	85.3
2. 0.5×10^{-4} M C_{16} Amine 0.5×10^{-4} M C_{16} Alcohol, C_{18} Acid C_{13} Phosphate	0.439	0.468	0.528	0.533	0.652		0.524	92.6
10 hours 80°C								
1. 0.5×10^{-4} M C_{16} Amine 0.5×10^{-4} M C_{16} Alcohol, C_{18} Acid C_{13} Phosphate	0.606	0.646	0.651	0.680	0.701		0.658	89.7

+ bracket figures not incorporated in average

APPENDIX G

EXPERIMENTAL ACTIVATION ENERGY FOR UNINHIBITED CORROSION

Linear Portion Only of Rate Curve

1. 60°

Weight-loss = 5.5%/14 hrs. = 0.393 weight %/hr.

Approximate sample weight = 5.5 gms.

Assume 100% Fe

$\therefore$ coupon = $\frac{5.5}{55.85}$ = 0.0985 moles of Fe

Corrosion rate = $\frac{0.393}{100} \frac{5.5}{55.85}$ = 0.000387 moles/hr.

ln rate = -8.21

2. $80^{\circ}C$

Weight-loss = 11.7%/9.33 hrs. = 0.911%/hr.

Corrosion rate = $\frac{0.911}{100}$ (0.0985) = 0.000897 moles/hr.

ln rate = -7.2

3. $90^{\circ}C$

Weight-loss = 8.9%/6.67 hrs. = 1.333%/hr.

Corrosion rate = $\frac{1.333}{100}$ (0.0985) = 0.001312 moles/hr.

ln rate = -6.64

Appendix G...continued

4. $95^{o}C$

Weight-loss = 11.9%/6.25 hrs. = 1.905 %/hr.

Corrosion rate = $\frac{1.905}{100}$ (0.0985) = 0.001875 moles/hr.

ln rate = -6.29

Arrhenius' Equation

$$k = Ae^{-E/RT}$$

$$\ln k = \ln A - E/RT$$

slope = -E/R

= 1.95/0.0003= 6500

E = 13,000 cals./mole

Experimental Activation Energy = 13,000 cals./mole

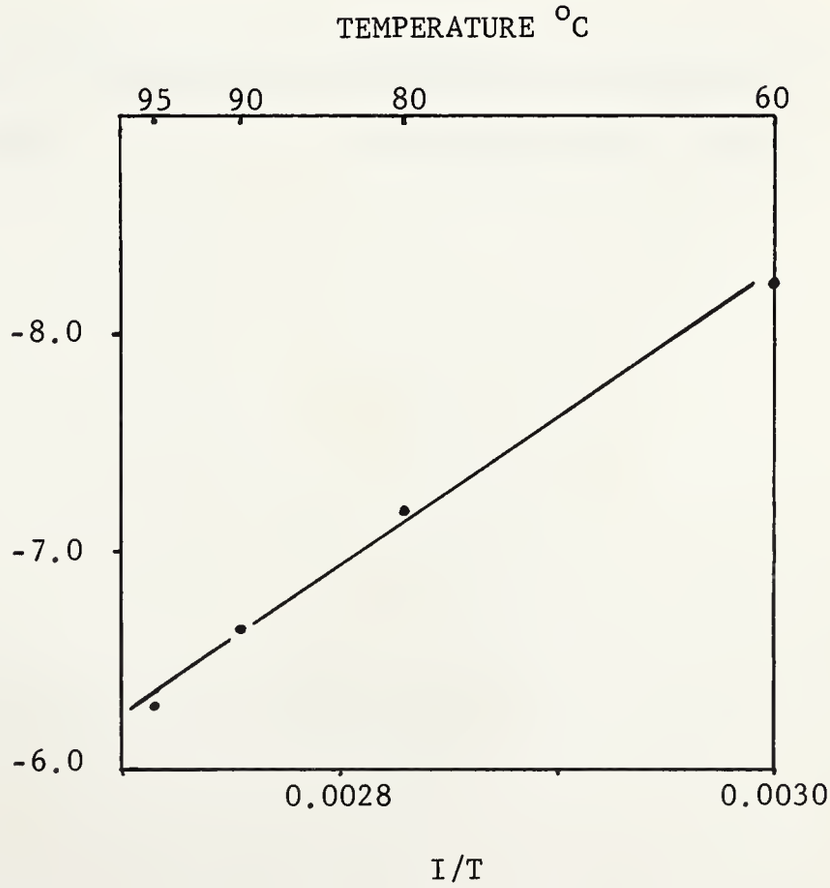

Fig. 28 Arrhenius Plot of Experimental Corrosion Rate Data

APPENDIX H

SURFACE TENSION STUDIES OF INHIBITED AND UNINHIBITED AQUEOUS HYDROCHOLORIC ACID SOLUTIONS, pH 1

The following calculations of surface tensions were made using the method outlined by Harkins and Brown (49) and using the following symbols:

ρ	- density of solution	gms/c.c.
d	- diameter	cm
r	- radius	cm
γ	- surface tension	dynes/cm
β	- drop volume correction constant	
$\psi(r/v^{1/3})$	- calculation constant	

Calibration Constant for conversion of micrometer screw units to drop volume — 1 micrometer unit = 0.02 c.c.

TABLE H-1

MELTING POINT DETERMINATIONS

Compound	Observed M.P. °C	Manufacturers M.P. °C	Published M.P. °C
Hexadecylamine	41.4	(1st component approx. 10%)	
	76-78	(2nd component approx. 90%)	
Stearic Acid	65-66		69.4
Hexadecylalcohol	45-47	48-49	49.3
Sodium Dodecycle Sulfate	decomposes		

Mono and Di Tridecyl Orthophosphate - commercial reagent, fluid at room temperature.

TABLE H-2

CALIBRATION OF DROP VOLUME SURFACE TENSION APPARATUS

	SOLUTION			
	Distilled H_2O 26° C	Distilled H_2O 60° C	pH1 HCl 24°C	pH1 HCl 60° C
Micrometer Units per drop	2.899	2.703	2.920	2.701
	2.893	2.701	2.909	2.703
	2.891	2.701	2.909	2.703
	2.892	2.702	2.913	2.706
	2.892	2.701	2.923	2.704
	2.897	2.695	2.908	2.695
	2.896	2.706	2.914	2.702
	2.894	2.706	2.908	2.705
	2.899	2.705	2.911	2.705
	2.897	2.705	2.908	2.702
	2.894	2.707	2.908	2.700
	2.897		2.934	
	2.891			
	2.892			
	2.890			
Average	2.894	2.704	2.914	2.703
Average drop volume (c.c.)	0.05788	0.05408	0.05828	0.05406
ρ Gms/c.c.	0.9968	0.9832	0.9973*	0.9832
Tip radius (cm)	0.1957	0.1957	0.1957	0.1957
$\psi(r/v^{1/3})$	0.506	0.517	0.504	0.517
β	0.649	0.646	0.6495	0.646
γ (dynes/cm)	71.1	65.6	71.3	65.6
γ (published)	71.8+	66.2+	72.1*	

\+ Handbook of Physics and Chemistry, Vol. 44, p. 2239

* See calculations on following page

Calculation of Surface Tension pH1 HCl

Aqueous HCl - pH1

acid used - 21 c.c. (concentrated) / 2 litres of solution

ρ acid = 1.1878 gms/c.c.

Strength - 37% HCl

21 c.c. acid = 21(1.1878) 0.37 gms HCl

= 4.61 gms/litre of solution

= 0.46 weight %

$20^{\circ}C$	
Weight Percent HCl	Surface Tension dynes/cm *
3.52	72.45
1.78	72.55

Extrapolated value of surface tension of 0.46 weight percent aqueous HCl

= 72.7 dynes/cm at $20^{\circ}C$

ρ H_2O, $20^{\circ}C$ = 0.9982 gms/c.c.

ρ 1% HCl, $20^{\circ}C$ = 1.003 gms/c.c.

Since the error introduced in γ calculations by the use of ρ H_2O instead of ρ HCl is within the experimental error, subsequently all calculations will use ρ H_2O at the temperature under consideration.

* Handbook of Physics and Chemistry, Vol. 44, page 2234

TABLE H-3

DETERMINATION OF C.M.C. OF HEXADECYL (C_{16}) AMINE

IN AQUEOUS HYDROCHLORIC ACID, pH1, 60°C

BY THE DROP VOLUME METHOD

	CONCENTRATION				
	1.5×10^{-4}M	1×10^{-4}M	0.83×10^{-4}M	0.5×10^{-4}M	0.33×10^{-4}M
Micrometer Units per drop	0.903	0.960	0.893	1.159	1.323
	0.900	0.945	0.905	1.108	1.377
	0.892	0.954	0.923	1.170	1.317
	0.906	0.945	0.939	1.132	1.367
	0.899	0.943	0.902	1.114	1.379
	0.899	0.950	0.943	1.146	1.379
	0.914	0.949	0.929	1.159	1.328
	0.887	0.954	0.960	1.140	1.299
	0.890	0.955	0.949	1.145	1.299
	0.892	0.960	0.961	1.169	
Average	0.898	0.9515	0.9304	1.144	1.341
Average drop volume (c.c.)	0.01796	0.01903	0.01861	0.02288	0.02682
ρ gms/c.c.*	0.9832				
Tip radius (cm)	0.1940	0.1940	0.1940	0.1940	0.1940
$\psi(r/V^{1/3})$	0.840	0.726	0.731	0.6825	0.648
β	0.6044	0.6061	0.6055	0.6120	0.6171
γ (dynes/cm)	23.6±0.4	24.8±0.1	24.4±0.4	29.7±0.5	34.4±0.6

* density of distilled water assumed to be sufficiently accurate for these and following determinations.

TABLE H-4

DETERMINATION OF THE C.M.C. OF AN EQUIMOLAR AQUEOUS ACID MIXTURE OF HEXADECYL AMINE AND ALCOHOL, STEARIC ACID AND DODECYL SODIUM SULFATE AT pH1 and 60°C BY THE DROP VOLUME METHOD

	CONCENTRATIONS (10^{-4}M)					
	1	0.83	0.5	0.33	0.12	0.077
Micrometer units per drop	0.946	0.922	1.074	0.983	1.622	1.794
	0.915	0.912	1.005	0.944	1.661	1.874
	0.959	0.978	1.059	0.983	1.547	1.800
	0.931	0.949	1.081	0.983	1.706	1.805
	0.945	0.965	1.059	0.964	1.669	1.818
	0.929	0.972	1.071	0.985	1.826	1.805
	0.946	0.915	1.011	0.999	1.586	1.843
	0.937	0.930	1.054	0.957	1.798	
	0.940	0.952	0.999	0.965	1.719	
				0.994	1.710	
Average	0.940	0.944	1.046	0.9757	1.684	1.820
Average drop volume (c.c.)	0.01880	0.01888	0.02092	0.01951	0.03368	0.03640
Tip radius (cm)	0.195	0.195	0.195	0.195	0.201	0.201
$\psi(r/v^{1/3})$	0.733	0.731	0.708	0.724	0.622	0.612
β	0.6053	0.6056	0.6084	0.6064	0.6215	0.6231
γ (dynes/cm)	24.4±0.4	24.6±0.7	27.1±1.0	25.3±0.8	41.2±3.3	44.6±1.0

B29815